ESCOLA DE CIÊNCIAS DA SAÚDE E DA VIDA
PROGRAMA DE PÓS-GRADUAÇÃO EM BIOLOGIA CELULAR E MOLECULAR
MESTRADO EM BIOLOGIA CELULAR E MOLECULAR

MARIO ALEJANDRO DUQUE VILLEGAS

Validação da enzima 5-enolpiruvilchiquimato-3-fosfato sintase (EPSP sintase) de *Mycobacterium smegmatis* como alvo molecular para o desenvolvimento de novas moléculas antimicobacterianas

Porto Alegre
2020

ESCOLA DE CIÊNCIAS DA SAÚDE E DA VIDA
PROGRAMA DE PÓS GRADUAÇÃO EM BIOLOGIA CELULAR E MOLECULAR
MESTRADO EM BIOLOGIA CELULAR E MOLECULAR

MARIO ALEJANDRO DUQUE VILLEGAS

Validação da enzima 5-enolpiruvilchiquimato-3-fosfato sintase (EPSP sintase) de *Mycobacterium smegmatis* como alvo molecular para o desenvolvimento de novas moléculas antimicobacterianas

Porto Alegre
2020

MARIO ALEJANDRO DUQUE VILLEGAS

Validação da enzima 5-enolpiruvilchiquimato-3-fosfato sintase (EPSP sintase) de *Mycobacterium smegmatis* como alvo molecular para o desenvolvimento de novas moléculas antimicobacterianas

Dissertação apresentada ao programa de Pós- Graduação em Biologia Celular e Molecular da Pontifícia Universidade Católica do Rio Grande do Sul como requisito parcial para obtenção do grau de Mestre em Biologia Celular e Molecular.

Orientador: Prof. Dr. Cristiano Valim Bizarro

Coorientador: Dr. Bruno Lopes Abbadi

Porto Alegre

2020

Ficha Catalográfica

V732v Villegas, Mario Alejandro Duque

Validação da enzima 5-enolpiruvilchiquimato-3-fosfato sintase (EPSP sintase) de Mycobacterium smegmatis como alvo molecular para o desenvolvimento de novas moléculas antimicobacterianas / Mario Alejandro Duque Villegas . – 2020.

87.

Dissertação (Mestrado) – Programa de Pós-Graduação em Biologia Celular e Molecular, PUCRS.

Orientador: Prof. Dr. Cristiano Valim Bizarro.
Co-orientador: Prof. Dr. Bruno Lopes Abbadi.

1. aroA. 2. Mycobacterium smegmatis. 3. MsEPSPS. 4. Vulnerabilidade. 5. CRISPRi. I. Bizarro, Cristiano Valim. II. Abbadi, Bruno Lopes. III. Título.

Elaborada pelo Sistema de Geração Automática de Ficha Catalográfica da PUCRS
com os dados fornecidos pelo(a) autor(a).
Bibliotecária responsável: Clarissa Jesinska Selbach CRB-10/2051

MARIO ALEJANDRO DUQUE VILLEGAS

Validação da enzima 5-enolpiruvilchiquimato-3-fosfato sintase (EPSP sintase) de *Mycobacterium smegmatis* como alvo molecular para o desenvolvimento de novas moléculas antimicobacterianas

Dissertação apresentada ao programa de Pós-Graduação em Biologia Celular e Molecular da Pontifícia Universidade Católica do Rio Grande do Sul como requisito parcial para obtenção do grau de Mestre em Biologia Celular e Molecular.

Banca Examinadora

Prof. Dr. Héctor Ricardo Morbidoni

Prof. Dr. Renata Medina da Silva

Prof. Dr. Luís Fernando Saraiva Macedo Timmers

Porto Alegre
2020

AGRADECIMENTOS

Quiero agradecer especialmente a el profesor Cristiano Valim Bizarro por haber respondido mi correo electrónico en el 2017, por haber aceptado a un estudiante al que no conocía físicamente.

También un reconocimiento especial a mi co-orientador Bruno Lopes Abbadi, por la paciencia y el constante apoyo, además porque aceptó el reto de orientar me cuando tenía mucho por aprender tanto en la parte técnica como comunicativa,

A los compañeros y amigos del CPBMF que ayudaron a soportar los momentos de incertidumbre y estrés, cuando creía que no iba a ser capaz de terminar este reto.

A Angélica y demás personas que fueron parte de mi familia en Brasil, que estuvieron ahí para ayudar constantemente.

A Dana mi mejor amiga y confidente, quien arduamente soportó las interminables horas de quejas, colapsos mentales, estrés y consejos para la toma de decisiones que han cambiado mi vida.

A mi familia que han sido fundamentales para mi formación como persona y profesional, por su apoyo financiero y emocional por ser mi motivación más grande y por los cuales quiero continuar este arduo proceso.

Al CAPES y BNDES por el apoyo financiero, sin los cuales desarrollar estudios de Maestría no hubiera sido posible.

RESUMO

A importância epidemiológica das bactérias do gênero *Mycobacterium* é indiscutível e a necessidade de encontrar novas moléculas que possam inibir o seu crescimento é urgente. A via do chiquimato, necessária para a síntese de importantes metabolitos em bactérias, representa um alvo para inibidores do crescimento da *Mycobacterium tuberculosis*. O gene *aroA* codifica a enzima 5-enolpiruvilchiquimato-3-fosfato sintase (EPSPS) que catalisa a sexta etapa da via do chiquimato. Neste estudo, combinamos nocaute de genes, e ensaios cinéticos para avaliar a essencialidade do gene *aroA* e experimentos de silenciamento gênico para avaliar a vulnerabilidade de seu produto protéico, EPSPS synthase de *Mycobacterium smegmatis* (*Ms*EPSPS), sob diferentes condições nutricionais. Demonstramos através de uma abordagem de nocaute gênico baseada na troca alélica, a essencialidade do *Ms*EPSPS sob condições nutricionais ricas e pobres. Ao realizar experimentos de complementação gênica com o tipo selvagem (WT) e versões mutantes pontuais do gene *aroA*, juntamente com ensaios cinéticos usando WT e proteínas recombinantes mutantes, demonstramos que a essencialidade do gene *aroA* depende da atividade da *Ms*EPSPS. Para avaliar a vulnerabilidade da *Ms*EPSPS, realizamos experimentos de silenciamento genico usando o sistema Clustered Regularly Interspaced Short Palindromic Repeats Interaction (CRISPRi). Os experimentos foram realizados tanto em meios ricos como definidos (pobres), usando três forças de repressão diferentes para o gene *aroA*. Apenas observamos um défice no crescimento quando as bactérias foram cultivadas em meios definidos sem suplementação de aminoácidos aromáticos, indicando assim que a vulnerabilidade do MsEPSPS depende das condições ambientais.

ABSTRACT

The epidemiological importance of bacteria from the genus *Mycobacterium* is indisputable and the necessity to find new molecules that can inhibit their growth is urgent. The shikimate pathway, required for the synthesis of important metabolites in bacteria, represents a target for inhibitors of *Mycobacterium tuberculosis* growth. The *aroA*-encoded 5-enolpyruvylshikimate-3-phosphate synthase (EPSPS) enzyme catalyzes the sixth step of the shikimate pathway. In this study, we combined gene knockout, gene knockdown and kinetic assays to evaluate *aroA* gene essentiality and the vulnerability of its protein product, EPSPS synthase from *Mycobacterium smegmatis* (*Ms*EPSPS), under different nutritional conditions. We demonstrate by an allelic exchange-based gene knockout approach the essentiality of *Ms*EPSPS under rich and poor nutritional conditions. By performing gene complementation experiments with wild-type (WT) and point mutant versions of *aroA* gene, together with kinetic assays using WT and mutant recombinant proteins, we show that *aroA* gene essentiality depends on *Ms*EPSPS activity. To evaluate *Ms*EPSPS vulnerability, we performed gene knockdown experiments using the Clustered Regularly Interspaced Short Palindromic Repeats interference (CRISPRi) system. The experiments were performed in both rich and defined (poor) media, using three different repression forces for *aroA* gene. We only observed growth impairment when bacteria were grown in defined medium without supplementation of aromatic amino acids, thereby indicating that *Ms*EPSPS vulnerability depends on the environment conditions.

LISTA DE FIGURAS

SUMÁRIO

1 INTRODUÇÃO

1.1 Epidemiologia da tuberculose humana

A tuberculose (TB) humana é uma doença infectocontagiosa causada principalmente pela bactéria da espécie *Mycobacterium tuberculosis*, que tem sido reconhecida como o patógeno microbiano que causou mais mortes na história da humanidade (1). O registro mais antigo de infecção na espécie humana é de aproximadamente 9.000 anos atrás no Mediterrâneo oriental, com incidentes no alvorecer da humanidade em culturas, épocas e áreas geográficas específicas, como nos egípcios e peruanos pré-colombianos (2,3).

Epidemiologicamente, a doença tornou-se mais importante a partir do século XIX, momento em que as taxas de transmissão e mortalidade estavam bastante elevadas, devido às condições de saúde da população, à aglomeração urbana e ao próprio desconhecimento da doença. Os primeiros registros da identificação clínica, patologia e termos relacionados à tuberculose, que ainda são usados até hoje, foram postulados na obra "*D'Auscultation mediate*" em 1819, de autoria de René Théophile Hyacinthe Laennec. (1).

O agente etiológico da doença, entretanto, ainda não havia sido identificado. Somente no final do século XIX, em 24 de março de 1882, que o Dr. Heinrich Hermann Robert Koch informou a "*Berlin Society of Physiology*" a identificação microbiológica e o meio de cultura específico do micro-organismo causador da TB pulmonar, chamado *Tuberkelvirus*, que um ano depois, em 1883, recebeu o nome científico *Mycobacterium tuberculosis* (3,4).

O último relatório global divulgado pela Organização Mundial da Saúde (OMS) (5) indicou que em 2019 aproximadamente 10 milhões de pessoas foram infectadas pelo patógeno, e que 1,2 milhão de indivíduos morreram em decorrência da doença. Estima-se que aproximadamente 95% das mortes causadas pelo bacilo ocorreram em países de baixa e média renda (países em desenvolvimento), evidenciando uma relação importante entre o estabelecimento da doença e os hábitos e condições de vida da população (alimentação, poluição, distribuição dos ambientes, consumo de álcool) (6). Entre as 10 milhões de pessoas infectadas, mais de 500 mil pessoas apresentaram tuberculose resistente aos dois principais medicamentos usados no tratamento, a isoniazida (INH) e a rifampicina (RIF), passando a ser classificada como

“tuberculose multirresistente a drogas” (MDR-TB). O desenvolvimento de cepas multirresistentes ameaça criar uma crise de segurança sanitária, já que prejudica as estratégias dos governos em atingir a meta de redução de 35% das mortes causadas pelo patógeno para o ano de 2020 (em relação ao ano de 2015) (7).

Diante desses dados, torna-se evidente que a TB é uma doença potencialmente mortal e que permanece bastante prevalente na população humana. Sendo assim, as pesquisas básicas acerca da biologia do patógeno continuam sendo essenciais para a compreensão do metabolismo da célula e para o desenvolvimento de novas ferramentas e estratégias de combate e diagnóstico da doença.

1.2 Microbiologia do *Mycobacterium tuberculosis*

O gênero *Mycobacterium* é constituído por aproximadamente 188 espécies e 5 subespécies, e é morfologicamente caracterizado por bacilos irregulares, com diâmetro entre 0,3-0,5 µm e com comprimento consideravelmente variável entre 1,5-4,0 µm. As bactérias desse gênero são resistentes à descoloração por ácido-álcool, aeróbicas facultativas, e possuem um conteúdo G+C bastante elevado no seu genoma (entre 62 e 70%) (8–10).

O *M. tuberculosis* tem sido descrito como um patógeno compulsório humano, já que depende unicamente desse hospedeiro para manter o seu ciclo de vida (11,12). Uma pessoa infectada e com a doença ativa transmite a bactéria através de aerossóis expelidos pelas vias áreas, principalmente ao tossir (**Figura 1**). Além disso, as micobactérias podem permanecer por longos períodos de tempo no ar em locais fechados, o que facilita a contaminação de indivíduos saudáveis que convivem com pessoas infectadas (13).

Figura 1- Ciclo de transmissão de *M. tuberculosis.*

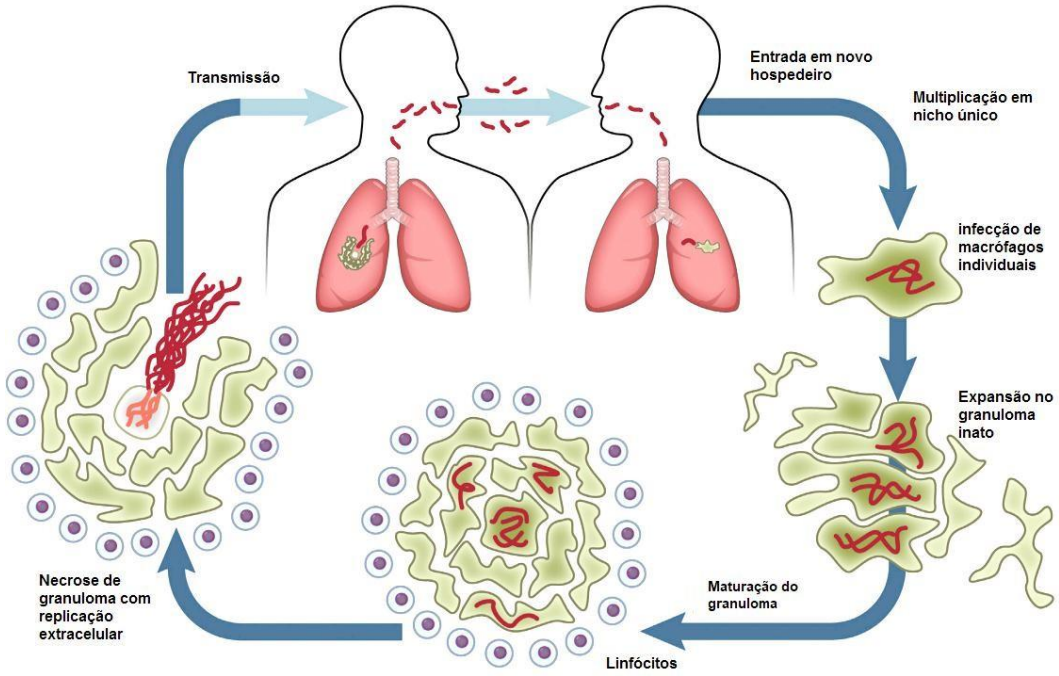

Fonte: Modificado de (14).

Uma das problemáticas mais amplamente abordadas no estudo da TB é a formação do granuloma, que é caracterizado por uma massa de tecido inflamado e infectado com bacilos viáveis e não-viáveis, os quais são circundados por macrófagos e linfócitos, que acabam formando uma espécie de “muro de proteção” para a micobactéria. Clinicamente, a TB é classificada de duas formas: 1) em doença **ativa** (pacientes que geralmente são sintomáticos e que transmitem a doença); e 2) infecção **latente** (LTBI, do inglês *latent tuberculosis infection*) (assintomática, não infecciosa, mas com risco variável de progressão para a tuberculose ativa) (15). A bactéria é capaz de resistir por meses, ou até anos, em um estado latente. Uma das preocupações acerca da LTBI é que os indivíduos infectados servem como potenciais reservatórios para a reativação e a transmissão da doença. Estima-se que até um terço da população mundial seja portadora da LTBI. Uma vez que o metabolismo da bactéria em estado de latência é pouco conhecido e mais difícil de ser estudado, poucos medicamentos foram desenvolvidos para agirem sobre o bacilo nesta situação (16,17).

1.3 Tratamento e resistência

O surgimento de cepas resistentes aos fármacos de primeira linha, a isoniazida (INH), a rifampicina (RIF), a pirazinamida (PIR) e o etambutol (EMB), que são medicamentos eficazes e amplamente utilizados no tratamento da doença, não é um evento recente. Entre 1993 e 1996, o centro de controle e prevenção de doenças dos Estados Unidos (CDC) relatou 1.457 casos de resistência à INH e RIF (18–20). Em 2012, essa mesma entidade aprovou a comercialização e o uso do fármaco Sirturo® (bedaquilina) para o tratamento de pacientes infectados com cepas MDR, renovando as esperanças para o combate à TB resistente (21).

O *M. tuberculosis* é capaz de desenvolver diferentes mecanismos de resistência para sobreviver à ação dos fármacos anti-TB, e por isso é essencial que o combate à doença seja feito na forma de terapia combinada. Um dos medicamentos de primeira linha, o pró-fármaco INH, por exemplo, precisa ser ativado pela enzima catalase-peroxidase, codificada pelo gene *katG* micobacteriano, para exercer seu efeito bactericida. Consequentemente, cepas de *M. tuberculosis* que carreguem mutações nesse gene desenvolvem resistência à INH, devido à redução da ativação do composto (22–24). Outras mutações amplamente documentadas na literatura científica são encontradas no gene *rpoB* e conferem resistência ao medicamento RIF (25).

Outro problema relacionado ao tratamento da TB está associado ao seu longo tempo de duração. Os medicamentos usados no tratamento de primeira linha , por exemplo, devem ser administrados por um mínimo de 6 meses (26), podendo se estender por até 18 meses (27). Sabe-se que esse fator contribui para o abandono precoce do tratamento por parte dos pacientes, uma vez que os sintomas da TB diminuem rapidamente já nos primeiros meses de intervenção.

Desde a geração dos primeiros compostos com atividade antimicobacteriana, tem-se dado preferência a moléculas que inibam a biossíntese de proteínas, ácidos micólicos, parede celular e ribossomos, já que esses são componentes essenciais para o desenvolvimento das micobactérias (28). Porém, como resposta aos desafios impostos pelas cepas MDR-TB, outras rotas metabólicas vêm sendo exploradas, como o metabolismo energético, especialmente a cadeia de transporte de elétrons, que tem sido postulado como uma via atrativa para o desenvolvimento de novos inibidores (29). Além disso, outras rotas metabólicas essenciais para o crescimento e a sobrevivência do patógeno têm sido estudadas, entre elas encontra-se o

metabolismo do ácido fólico (30), a rota das purinas (31), a biossíntese de nucleotídeos (32) e a via do ácido chiquímico. Esta última tem se tornado uma rota interessante primeiramente por ser essencial à sobrevivência das micobactérias e, também, por estar ausente em humanos, o que diminuiria as chances de efeitos adversos por possíveis inibidores das enzimas da via (33).

1.4 Identificação e desenvolvimento de compostos antimicrobianos

A identificação de novos compostos com uma atividade antibacteriana (bactericida ou bacteriostática) satisfatória pode ser feita por duas abordagens principais (**Figura 2**). A metodologia clássica segue o caminho da droga para o alvo (em inglês *drug-to-target*), já que essa abordagem pode ser feita, por exemplo, a partir de extratos brutos de plantas com atividade medicinal, ou também a partir de bibliotecas de compostos químicos com atividade ainda desconhecida.

Figura 2- Abordagens para a descoberta de novos compostos para tratar a tuberculose**.**

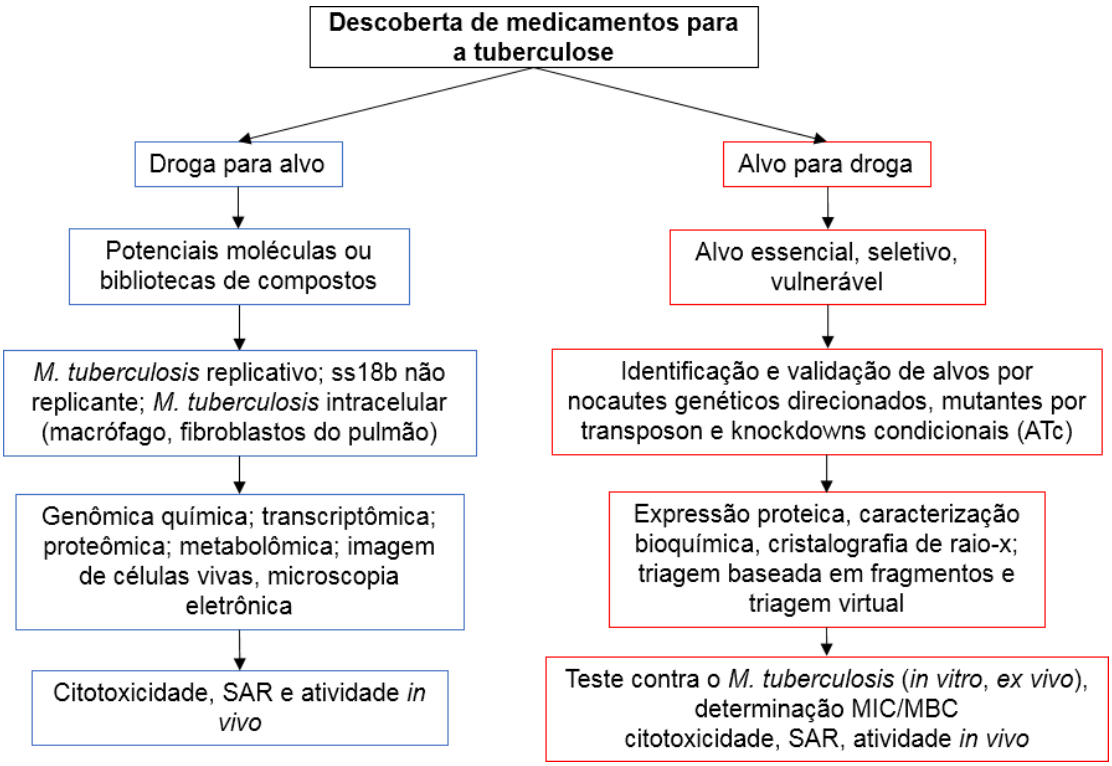

Fonte: Modificado de (34,35).
Nota: A siglas SAR significa ‘relação estrutura-atividade’ (do inglês *structure-activity relationship*) e ATc significa “anidrotetraciclina”.

Essa metodologia é conhecida como **abordagem fenotípica** e tem como etapas principais: 1) a seleção de compostos quimicamente diversos, a partir de bibliotecas, que podem, ou não, ter atividade antimicobacteriana previamente conhecida; 2) ensaios de atividade *in vitro* contra o *M. tuberculosis* em estado replicativo, por meio de ensaios de determinação da concentração inibitória mínima (CIM) e, posteriormente, em modelos de infecção em células hospedeiras (ex.: linhagem de macrófagos murinos); 3) testes em modelos animais de infecção pelo *M. tuberculosis*; e 4) determinação do mecanismo de ação e elucidação do alvo molecular (34). Um dos compostos que foi selecionado a partir dessa metodologia foi a piridomicina, um produto natural que tem como alvo a enzima *InhA* (o mesmo alvo da isoniazida), e que exerce um efeito bactericida sobre o *M. tuberculosis* (34). Em anos mais recentes, a triagem fenotípica voltou a ganhar força, reapresentada com técnicas de *high-throughput screening* chamada estratégia neoclássica, já que mistura a abordagem fenotípica com novas técnicas de biologia molecular (36).

Embora a maioria dos fármacos anti-TB tenha sido identificada por essa metodologia, a abordagem baseada no alvo (do inglês *target-to-drug*) ganhou força no final dos anos 90 e contribuiu para o desenvolvimento de diferentes técnicas de biologia molecular, química medicinal, entre outras (37). O sequenciamento completo do genoma de *M. tuberculosis* permitiu aos pesquisadores identificar genes (e proteínas) essenciais para o metabolismo do patógeno, que podem servir de alvos para o planejamento racional de inibidores (38). No entanto, sabe-se que essa abordagem apresenta diversas limitações, incluindo a dificuldade em selecionar alvos essenciais para o contexto de infecção e a falta de transposição da atividade observada *in vitro*, contra proteínas isoladas, para a atividade contra células bacterianas vivas (26,35). Entre as etapas da abordagem baseada no alvo, está incluída a própria identificação e validação dos alvos moleculares, que sejam necessariamente essenciais para a sobrevivência do bacilo, e vulneráveis à ação de inibidores.

1.5 Identificação e validação de novos alvos moleculares

A primeira etapa para o desenvolvimento de compostos antimicrobianos baseados no alvo consiste na identificação de rotas metabólicas ou, mais especificamente, de proteínas que sejam vitais para a sobrevivência do bacilo. Um

dos conceitos mais amplamente utilizados na identificação de alvos promissores é a essencialidade, na qual busca-se um gene, e seu produto proteico correspondente, sem o qual a micobactéria não é capaz de manter o seu metabolismo. A avaliação dessa essencialidade pode ser feita por diferentes estratégias de genética reversa ou direta, que incluem o nocaute gênico direcionado por recombinação homóloga, a partir de transdução de fago, mutagênese de alta densidade mediada por transposons e a mutagênese por troca alélica baseada em plasmídeos (*lacZ*, *sacB*, *rpsL* e *galK*) (34,39). Estas ferramentas podem ser usadas tanto em contextos *in vitro* de crescimento, para identificar condições de cultivo nas quais o gene torna-se essencial, por exemplo, ou *in vivo*, os quais simulam o fenômeno da infecção (ex.: modelo de infecção de camundongo) e permitem avaliar genes que são importantes para o ciclo de vida no hospedeiro.

Embora por muitos anos os pesquisadores tenham focado na busca de alvos essenciais, hoje já se sabe que alguns genes/proteínas que são, de fato, essenciais, não são, ao mesmo tempo, vulneráveis (40). A vulnerabilidade está vinculada à quantidade de inibição necessária para a observação de um efeito deletério sobre o crescimento de um organismo (26). Alvos proteicos vulneráveis, portanto, são aqueles em que a incompleta inibição da sua atividade produz um fenótipo letal. Por exemplo, um alvo considerado vulnerável é o exportador de monomicolato de trealose (denominado MmpL3), que atua no transporte do precursor monomicolato de trealose (TMM) para fora da célula (41). A identificação desses alvos é feita principalmente por meio de técnicas de silenciamento gênico, que consistem na redução condicional da expressão de um gene de interesse e na observação do fenótipo resultante; assim sendo, genes que requerem uma redução incompleta da expressão são considerados vulneráveis. Diversas ferramentas já foram desenvolvidas para essa finalidade, sendo que, a mais recente, está baseada no sistema CRISPR-Cas9 (34).

Originalmente o sistema CRISPR-Cas9 (acrônimo oriundo das palavras *Clustered Regularly Interspaced Short Palindromic Repeats*) era composto por uma enzima com atividade de endonuclease, chamada de Cas9, capaz de realizar quebras de fita-dupla no genoma de interesse para fins de edição gênica. A Cas9 é direcionada para o gene de interesse através da interação com o RNA guia (do inglês *guide RNA*, ou *gRNA*), que é capaz de fazer um pareamento de bases Watson-Crick com uma das fitas de DNA do gene-alvo (41).

No entanto, Rock e colaboradores, em 2017, desenvolveram uma variação deste sistema, no qual se utilizou uma versão inativa da enzima Cas9 (do inglês *dead*-Cas9, ou dCas9) que é incapaz de realizar quebras de fita-dupla no DNA. Os pesquisadores descobriram que a expressão da enzima inativa de *Streptococcus thermophilus* ($dCas9_{Sth1}$) não causa efeitos proteotóxicos nas micobactérias, como observado anteriormente para a mesma enzima derivada de *S. pyogenes*. O uso da $dCas9_{Sth1}$ permite silenciar a expressão de genes através da ligação da proteína ao complexo gRNA-DNA (**Figura 3**). A enzima permanece "estacionada" sobre o DNA marcado pelo gRNA, causando um impedimento físico da passagem da RNA polimerase pela fita de DNA (alongamento da transcrição). O sistema foi denominado de interferência mediada por CRISPR (*CRISPRi*) e já foi satisfatoriamente testado em micobactérias (41,42).

Figura 3- Interação do Sistema de CRISPRi com o DNA-alvo.

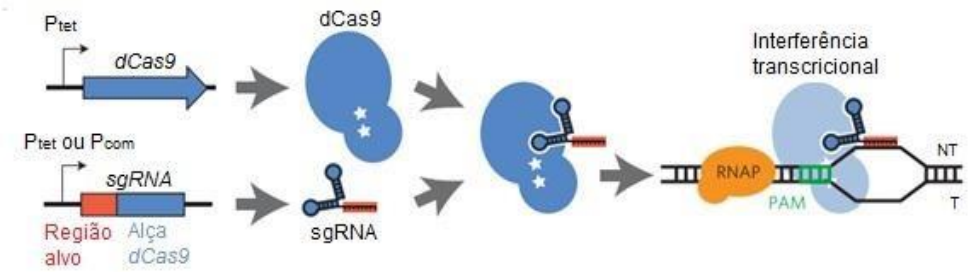

Fonte: Adaptado de (41).
Legenda: RNAP = RNA polimerase. gRNA = RNA guia. PAM = motivo adjacente ao protoespaçador. NT: não template. T: template.

A vulnerabilidade de diferentes alvos moleculares tem sido avaliada utilizando esse sistema. Um dos primeiros alvos avaliados com o sistema CRISPRi foi o gene *mmpL3*: testes *in vitro* e *in vivo* refletiram o declínio da exportação de ácido micólico, produzindo uma atenuação no crescimento das bactérias, propondo o alvo como fortemente vulnerável (43). Outro alvo avaliado por esse sistema foi o gene *sepF*, que codifica para a enzima de divisão celular SepF, que, quando silenciada, afeta o crescimento bacteriano e promove mudanças morfológicas no bacilo, indicando a possível vulnerabilidade do alvo (42).

1.6 Rota do ácido chiquímico

De acordo com a literatura, a rota do ácido chiquímico é considerada uma via atraente para o desenvolvimento de novos agentes antimicrobianos, uma vez que é essencial para o crescimento de algas, plantas, fungos e, também, de bactérias. A via está ausente na maioria dos animais, incluindo os mamíferos, o que favorece o desenvolvimento de inibidores seletivos para as enzimas de bactérias patogênicas, como é o caso do *M. tuberculosis* (44).

Nas bactérias, a rota ocorre em sete etapas e inicia pela reação de condensação entre o substrato fosfoenolpiruvato (**PEP**) e a D-eritrose 4-fosfato (**E4P**) pela enzima DAHP sintase. Após sete etapas enzimáticas, ocorre a formação de ácido corísmico, que atua como uma molécula precursora para a biossíntese de aminoácidos aromáticos (triptofano, tirosina e fenilalanina), além de poder dar origem às naftoquinonas, menaquinonas, micobactinas, folatos e ubiquinonas (45,46). Para que estes produtos essenciais sejam sintetizados a partir do corismato, é necessária a presença das enzimas **DAHP sintase** (3-deoxi-d-arabino-heptulosonato-7-fosfato sintase), **DHQ sintase** (3-desidroquinato sintase), **DHQ desidratase** (3-desidroquinato desidratase), **chiquimato desidrogenase**, **chiquimato quinase**, **EPSP Sintase** (5-enolpiruvilchiquimato-3-fosfato sintase) e a **corismato sintase** (**Figura 4**) (47).

Figura 4- Rota do ácido chiquímico.

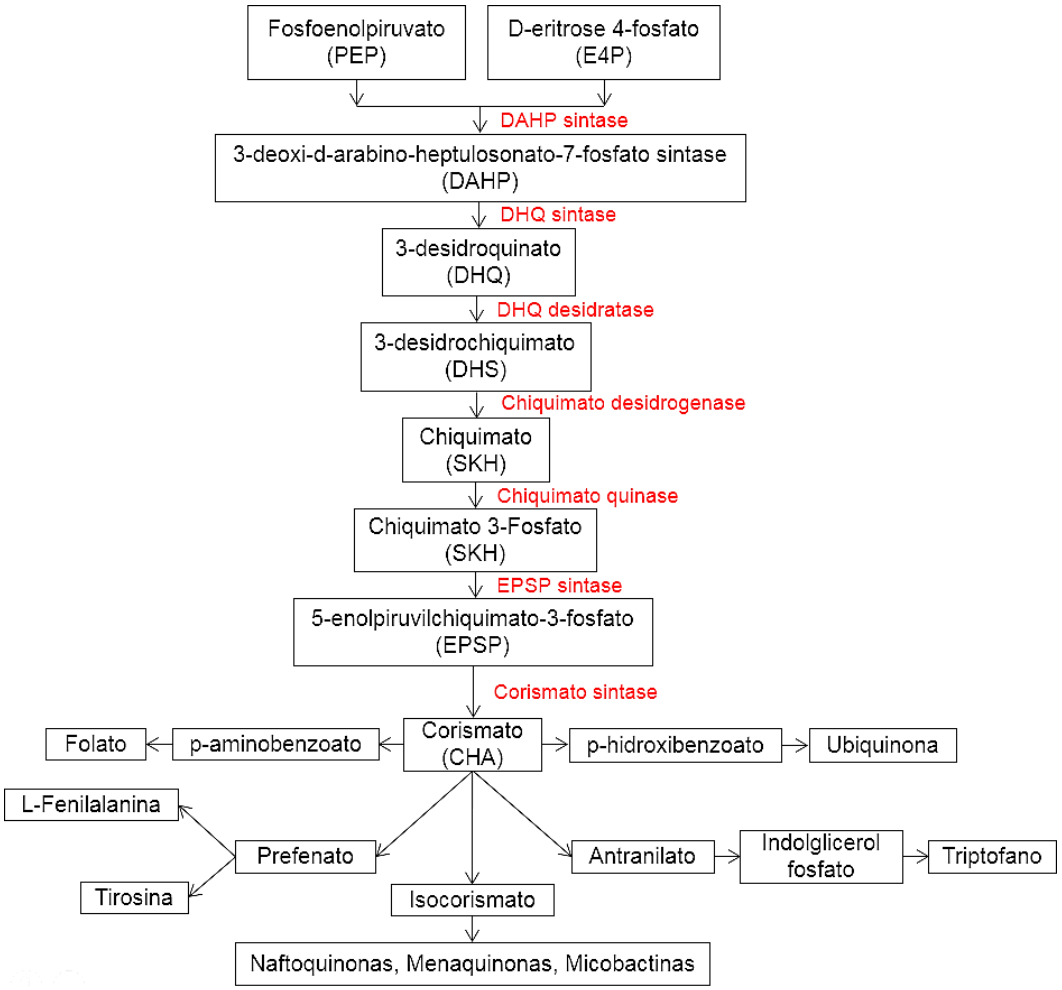

Fonte: Adaptado de (47).

Para estudar a rota é importante conhecer a organização dos genes *aro*, que codificam as sete enzimas da rota do ácido chiquímico e que, embora conservados entre as micobactérias, apresentam algumas diferenças (47). Em *M. tuberculosis*, por exemplo, já foi identificado o gene *aroK* como essencial, além disso os genes *aroCKBQ* estão agrupados em um único operon (**Figura 5**). Já o gene *aroE* encontra-se em um operon com outros quatro genes (Rv2551c, Rv2553c, Rv2554c e *alaS*) com funções não relacionadas, enquanto o gene *aroA* pertence a um operon bicistrônico juntamente com o gene Rv3228. O gene *aroG* seria o único gene *aro* monocistrônico, ou seja, que não está contido em um operon. O gene *aroQ* de *M. smegmatis*, entretanto, não está contido no operon *aroCKBQ*; este gene encontra-se em outra região do genoma e não faz parte de um operon (47).

Figura 5- Organização dos genes aro em micobactérias e seus respectivos operons

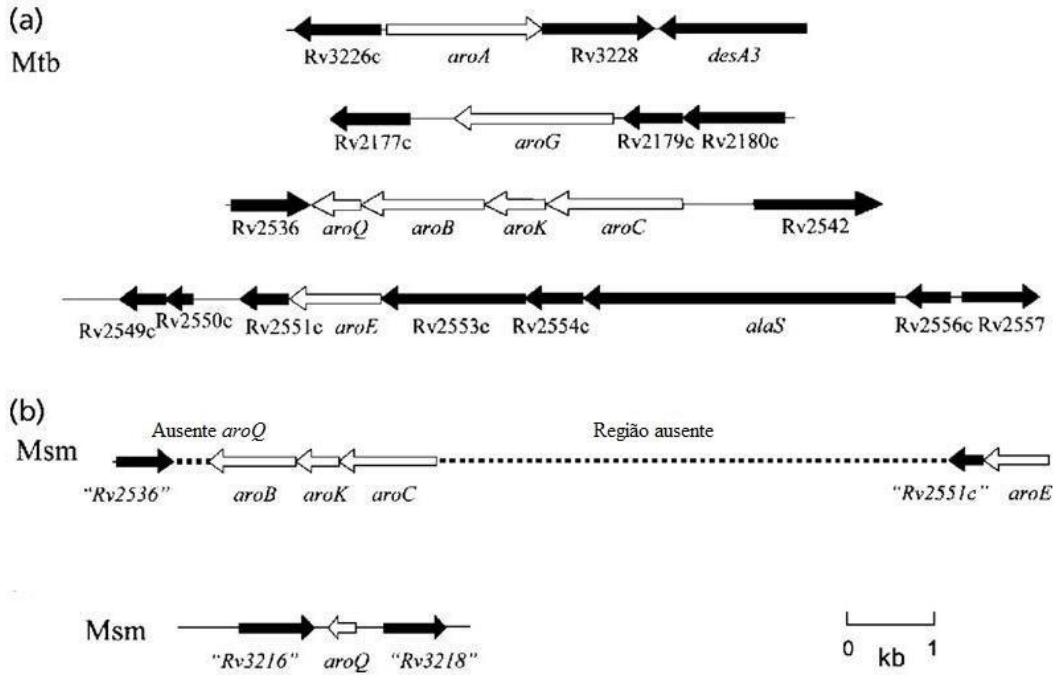

Fonte: Adaptado de (47).
Nota: Organização dos genes nas micobactérias (a) *M. tuberculosis* e (b) *M. smegmatis*.

Em 2003, Sassetti e colaboradores (48) e, posteriormente, Griffin e colaboradores em 2011 (49), relataram a essencialidade dos “genes aromáticos” *aro* que codificam as enzimas da via (**Tabela 1**). Sendo assim, assume-se que a rota é essencial para o crescimento de *M. tuberculosis* e que as enzimas são vistas como alvos interessantes para o desenvolvimento de compostos com atividade antimicobacteriana (47).

Tabela 1 - Descrição genética das sete proteínas envolvidas na via do ácido chiquímico de *M. tuberculosis* e *M. smegmatis.*

Enzima	*M. tuberculosis*			*M. smegmatis*		
	Locus	**Gene**	**Tamanho (pb)**	**Locus**	**Gene**	**Tamanho (pb)**
DAHP Sintase	Rv2178c	*aroG*	1.389	MSMEG_4244	MSMEG_4244	1.395
DHQ Sintase	Rv2538c	*aroB*	1.089	MSMEG_3033	*aroB*	1.122
DHQ Desidrogenase	Rv2537c	*aroD*	444	MSMEG_1922	*aroQ*	438
Chiquimato Desidrogenase	Rv2552c	*aroE*	810	MSMEG_3028	*aroE*	831
Chiquimato Quinase	Rv2539c	*aroK*	531	MSMEG_0453	*aroK*	513
EPSP Sintase	Rv3227	*aroA*	1.353	MSMEG_1890	*aroA*	1.332
Corismato Sintase	Rv2540c	*aroF*	1.206	MSMEG_3030	*aroC*	1.200

Nota: Genes descritos como essenciais para o crescimento *in vitro* do *M. tuberculosis*, de acordo com a técnica de mutagênese por transposon (48,49).

1.6.1 EPSP sintase

A enzima **5-enolpiruvilchiquimato-3-fosfato sintase** (**EPSP sintase**; EC 2.5.1.19) de *M. tuberculosis*, codificada pelo gene ***aroA*** (**Tabela 1**), é uma enzima monomérica que apresenta um peso molecular de 46,4 kDa. Estruturalmente essa enzima tem dois domínios, formados por três cópias de unidades βαβαββ e com o sítio ativo próximo ao segmento de cruzamento entre os domínios (**Figura 6**) (44,45,50).

Figura 6- Estrutura tridimensional da enzima EPSP sintase de *M. tuberculosis* acoplada ao S3P.

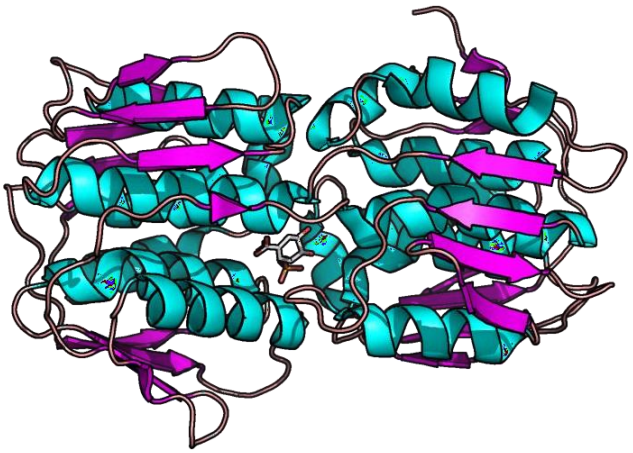

Fonte: Obtido a partir da base de dados *Protein Data Bank* (RCSB-PDB).
Nota: Código de acesso da estrutura cristalográfica: 2O0B.

A EPSP sintase participa da sexta reação da rota do ácido chiquímico (**Figura 4**) e catalisa a transferência reversível da porção carboxivinil, do substrato fosfoenolpiruvato (PEP), para a hidroxila-5 do chiquimato-3-fosfato (S3P), formando o produto enolpiruvilchiquimato-3-fosfato (EPSP) e fosfato inorgânico (**Figura 7**) (51).

Figura 7- Reação catalisada pela enzima EPSP sintase.

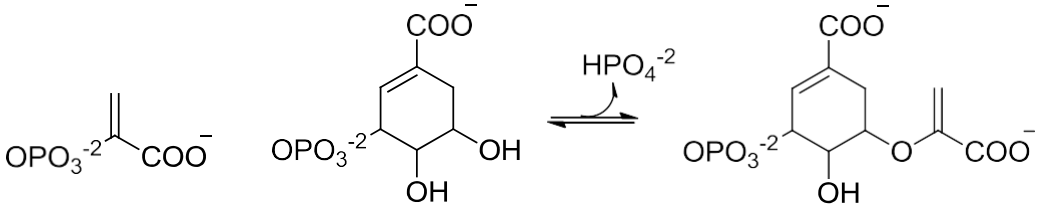

Fonte: Baseado em (52).

Diferentes estudos já apontaram a importância funcional da EPSP sintase para a sobrevivência das bactérias. A deleção do gene *aroA* causou, por exemplo, a atenuação da virulência de cepas de *Streptococcus pneumoniae* (53) e *Bordetella bronchiseptica* (54), além de *Salmonella typhimurium,* espécies do gênero *Aeromonas*

e Shigella, as quais se tornam incapazes de sobreviver *in vivo* e de causar infecção (55).

Sabe-se, até o presente momento, que a EPSP sintase é o único alvo celular para o famoso herbicida **glifosato**, comercialmente conhecido como *RoundUP* e *Compare-N-Save* (56). Esse composto liga-se ao complexo enzima-S3P, fazendo uma ligação competitiva com o substrato PEP (44) e, consequentemente, inibindo a atividade enzimática (57). Desde que foi comprovada a atividade inibitória do glifosato sobre as bactérias, diferentes cepas resistentes ao composto já foram identificadas. Por exemplo, na *E. coli* já foram identificadas as mutações G96A e A183T na enzima, que, quando estão presentes, tornam a bactéria insensível ao glifosato (58).

Em 2013, Ramachandran e colaboradores (40) realizaram estudos de inibição da EPSP sintase de *E. coli* e de *M. tuberculosis* com o glifosato. Os pesquisadores observaram que os valores de IC_{50} para a EPSP sintase de *M. tuberculosis* foram cerca de 86 vezes maiores (IC_{50} = 260 µM), do que para o ortólogo de *E. coli* (3 µM), sugerindo uma menor afinidade do glifosato pela enzima micobacteriana. Além disso, os autores fizeram predições *in silico* da possível concentração inibitória mínima (MIC) e do efeito do silenciamento condicional para *M. tuberculosis*. Os resultados obtidos sugeriram uma MIC consideravelmente alta (30 mg/mL), e que o silenciamento incompleto desse gene (<100%) não causaria qualquer impacto sobre o crescimento do bacilo. Esses dados, entretanto, ainda precisam ser comprovados experimentalmente.

Um dos fatos mais importantes a respeito da EPSP sintase é a sua plasticidade estrutural, já que a enzima pode transitar entre cinco estados conformacionais diferentes. Estudos de dinâmica molecular mostraram que a enzima pode transitar entre dois estados abertos, um entreaberto e dois fechados, e sabe-se que a flexibilidade estrutural é importante como um mecanismo para se adaptar a diferentes tipos de ligante (59).

Conhecer as possíveis conformações da EPSP sintase é importante para identificar os resíduos de aminoácidos que são essenciais para manter a conformação e a atividade enzimática. Sabe-se que a mudança do resíduo aspartato 49 por uma alanina (D49A) na enzima de *E. coli*, por exemplo, causa uma redução de 21.000 vezes na atividade específica da enzima e tem um efeito deletério sobre o crescimento bacteriano (52). O mesmo fenômeno é proposto para mutações nos aminoácidos

hidrofóbicos, como valina, isoleucina, leucina, metionina, fenilalanina, tirosina e triptofano na enzima de *M. tuberculosis* (59).

Embora as evidências apontem que a enzima EPSP sintase micobacteriana é essencial para a sobrevivência desses organismos, e que pode vir a ser um alvo atraente para o desenvolvimento de novos inibidores antimicobacterianos (40,45,50,60–62), nenhum trabalho reportou ainda o nocaute direcionado do gene *aroA*, de forma a comprovar essa característica. Além disso, ainda não foram demonstrados quais resíduos de aminoácidos são importantes para a atividade enzimática da EPSP sintase, de forma que seja possível projetar inibidores capazes de interagir com tais resíduos e abolir a atividade da enzima. Sendo assim, um dos objetivos do presente projeto foi realizar o nocaute do gene *aroA* de *M. smegmatis* e a complementação com o gene selvagem e com mutantes estruturais da enzima *Ms*EPSPs. O *M. smegmatis* vem sendo usado por diferentes grupos de pesquisa como uma micobactéria-modelo, uma vez que apresenta algumas características que facilitam o seu manuseio, como o tempo de geração mais curto (entre 3 e 4 horas) em relação ao *M. tuberculosis,* e a ausência de virulência, o que dispensa a necessidade de um laboratório de biossegurança nível 3 para manipulá-la. Além disso, a rota do chiquimato está conservada no *M. smegmatis*, ainda que existam algumas diferenças na distribuição dos genes *aro* em relação ao *M. tuberculosis*. Além de avaliar a complementação funcional das mutantes estruturais, os parâmetros cinéticos de cada enzima foram determinados por meio de ensaios de atividade enzimática *in vitro*. Juntos esses experimentos permitiram avaliar a essencialidade não só do gene *aroA*, mas também de resíduos específicos da enzima. Por fim, diferentes experimentos de silenciamento gênico foram realizados utilizando a técnica CRISPRi, que permitiram acessar a vulnerabilidade da enzima *Ms*EPSPS em diferentes condições de cultivo *in vitro*.

2 OBJETIVOS

2.1 Geral

Validar a enzima 5-enolpiruvilchiquimato-3-fosfato sintase de *M. smegmatis* (*Ms*EPSPs) como um alvo molecular para o desenvolvimento de novas moléculas antimicobacterianas.

2.2 Específicos

1. Avaliar a essencialidade do gene *aroA* de *M. smegmatis* por meio de experimentos de nocaute gênico.

2. Testar a essencialidade de resíduos específicos da enzima *Ms*EPSPs por meio de experimentos de complementação gênica em *M. smegmatis*.

3. Avaliar a vulnerabilidade do gene *aroA* de *M. smegmatis* por meio de experimentos de silenciamento condicional pelo sistema CRISPRi.

4. Clonar, expressar e purificar mutantes estruturais recombinantes da enzima *Ms*EPSPs em células de *Escherichia coli*.

5. Avaliar e comparar o crescimento das cepas mutantes para o gene *aroA* em relação à cepa selvagem de *M. smegmatis*.

6. Determinar os parâmetros cinéticos (K_M, K_{cat}) de alguns mutantes estruturais da *Ms*EPSPs por meio de ensaios de atividade enzimática *in vitro*.

7. Correlacionar os dados de atividade enzimática *in vitro* das mutantes estruturais com a complementação dos genes mutantes em células de *M. smegmatis*.

3 ARTIGO CIENTÍFICO

Evaluating *aroA* gene essentiality and EPSP synthase vulnerability in *Mycobacterium smegmatis* under different nutritional conditions

Mario Alejandro Duque-Villegas[a, b], Bruno Lopes Abbadi[a], Paulo Ricardo Romero[a], Luiza Galina[a], Pedro Ferrari Dalberto[a, b], Valnês da Silva Rodrigues-Junior [a], Candida Deves Roth[a], Raoní Scheibler Rambo[a], Eduardo Vieira de Souza[a, b], Marcia Alberton Perello[a], Pablo Machado[a, b], Luiz Augusto Basso[a, b,c], Cristiano Valim Bizarro[a, b]*

[a] Instituto Nacional de Ciência e Tecnologia em Tuberculose (INCT-TB), Centro de Pesquisas em Biologia Molecular e Funcional (CPBMF), Pontifícia Universidade Católica do Rio Grande do Sul (PUCRS), 92A TECNOPUC, 4592 Av. Ipiranga 6681, 90616-900, Porto Alegre, Brazil.

[b] Programa de Pós-Graduação em Biologia Celular e Molecular, PUCRS, Porto Alegre, Brazil

[c] Programa de Pós-Graduação em Medicina e Ciências da Saúde, PUCRS, Porto Alegre, Brazil

*Corresponding author: cristiano.bizarro@pucrs.br (C. V. Bizarro)

Abstract

The epidemiological importance of bacteria from the genus *Mycobacterium* is indisputable and the necessity to find new molecules that can inhibit their growth is urgent. The shikimate pathway, required for the synthesis of important metabolites in bacteria, represents a target for inhibitors of *Mycobacterium tuberculosis* growth. The *aroA*-encoded 5-enolpyruvylshikimate-3-phosphate synthase (EPSPS) enzyme catalyzes the sixth step of the shikimate pathway. In this study, we combined gene knockout, gene knockdown and kinetic assays to evaluate *aroA* gene essentiality and the vulnerability of its protein product, EPSPS synthase from *Mycobacterium smegmatis* (*Ms*EPSPS), under different nutritional conditions. We demonstrate by an allelic exchange-based gene knockout approach the essentiality of *Ms*EPSPS under rich and poor nutritional conditions. By performing gene complementation experiments with wild-type (WT) and point mutant versions of *aroA* gene, together with kinetic assays using WT and mutant recombinant proteins, we show that *aroA* gene essentiality depends on *Ms*EPSPS activity. To evaluate *Ms*EPSPS vulnerability, we performed gene knockdown experiments using the Clustered Regularly Interspaced Short Palindromic Repeats interference (CRISPRi) system. The experiments were performed in both rich and defined (poor) media, using three different repression forces for *aroA* gene. We only observed growth impairment when bacteria were grown in defined medium without supplementation of aromatic amino acids, thereby indicating that *Ms*EPSPS vulnerability depends on the environment conditions.

Importance

We evaluated both gene essentiality and target vulnerability of the enzyme that catalyzes the sixth step of the shikimate pathway, the *aroA*-encoded 5-enolpyruvylshikimate-3-phosphate synthase from *Mycobacterium smegmatis* (MsEPSPS). Combining gene knockout experiments and kinetic assays, we established a causal link between *aroA* gene essentiality and the biological function of EPSPS protein, which we advocate is an indispensable step for target validation. Moreover, we characterized *Ms*EPSPS vulnerability under different nutritional conditions and found it is a vulnerable target only when *M. smegmatis* is grown under poor nutritional conditions without supplementation with aromatic amino acids. Based on our findings, we suggest that gene essentiality information should be obtained from gene knockout experiments and not knockdown approaches, as even low levels of a protein after gene silencing can lead to a different growth phenotype when compared to that under its complete absence, as was the case with *aroA* and *Ms*EPSPS in our study.

Keywords

Gene silencing, Chorismate, Essentiality, Vulnerability, CRISPRi, Molecular genetics.

INTRODUCTION

Human tuberculosis (TB) is an important infectious disease that continues to be a public health threat worldwide. Despite the joint global efforts to lower TB burden, which resulted in a 6.3% and 11% cumulative decline in incidence and mortality, respectively, between 2015 and 2018, the End TB Strategy milestones for 2020 are far from being reached [1]. According to the last World Health Organization (WHO) TB report, around 10.0 million people developed the disease, and 1.2 million HIV-negative individuals died from it in 2018 [1]. In humans, the acid-fast *Mycobacterium tuberculosis* bacilli is the main causative agent of pulmonary TB, a debilitating condition that is fatal without treatment [1,2]. Although TB is considered a curable disease, with a success rate of approximately 85% for drug-susceptible strains, the spread of multidrug-resistant and rifampicin-resistant TB (MDR/RR-TB) poses a challenge to the current first-line treatment [1]. Resistance cases of TB have been documented since the very beginning use of streptomycin as the first anti-TB monotherapy in 1943 [3, 4]. Therapies for MDR/RR-TB are complex, more expensive, longer, and more toxic, when compared to those for drug-susceptible TB, and it is estimated that only 56% of MDR-TB cases reach cure [1,5].

The spread of resistant strains is related to the acquisition of multiple molecular mechanisms that allows *M. tuberculosis* evade the action of anti-TB drugs, mostly by mutations on drug targets [6]. Therefore, the development of new anti-TB drugs having new mechanisms of action are needed. As the number of molecular targets of current bacterial agents are limited [7], there is a growing interest in finding and validating new molecular targets for drug development. Apart from being essential, a drug target should be vulnerable, which means that

the incomplete inhibition of its activity is sufficient to produce a lethal phenotype [8]. Some genes/proteins were found to be essential but not vulnerable, prompting the need to use molecular genetic tools to study target vulnerability as part of the target validation process [9,10].

The shikimate pathway is considered an attractive target for the development of rational-based new antimicrobial agents. It is essential for the growth of bacteria, but absent in most animals, including mammals, favoring the development of selective inhibitors for pathogenic bacteria [11,12]. This pathway is composed by seven different enzymatic steps, leading to the production of chorismate, which is a precursor of naphthoquinones, menaquinones and mycobactins as well as folates, ubiquinones, tryptophan, tyrosine and phenylalanine [11,13,14].

The 5-enolpyruvylshikimate-3-phosphate synthase (EPSPS; EC 2.5.1.19) is the sixth enzyme of the shikimate pathway. EPSPS is coded by *aroA* gene and catalyzes the transfer of the carboxyvinyl portion of the phosphoenolpyruvate substrate (PEP) to the carbon-5 hydroxyl group of shikimate 3-phosphate (S3P) to form the enolpyruvyl shikimate-3-phosphate product (EPSP) [15]. The *aroA* gene was found to be essential for growth or virulence for many bacterial species, such as *Streptococcus pneumoniae*, *Bordetella bronchiseptica*, *Salmonella typhimurium* and species of the genus *Aeromonas* and *Shigella* [16,17]. However, the vulnerability of EPSPS as a drug target was not experimentally studied yet.

In this study, we used *Mycobacterium smegmatis* as a model organism to evaluate the essentiality of *aroA* gene and the vulnerability of its protein product

(*Ms*EPSPS). The *aroA* gene was knocked out in allelic exchange experiments and found to be essential for *M. smegmatis* growth under the conditions tested. We also evaluated the ability of a wild-type (WT) *aroA* gene or *aroA* alleles containing point mutations to complement the knockout (KO) *aroA* strain. Specifically, we found two EPSPS amino acid residues as essential (R134 and E321). Mutated versions of recombinant *Ms*EPSPS were expressed, purified and their kinetic activities characterized. We found that recombinant R134 and E321 mutants have diminished EPSPS enzyme activity. Our results suggest that the *aroA* essentiality under our experimental conditions depends on the EPSPS activity of its protein product. Moreover, using the CRISPRi system [18], we evaluated EPSPS vulnerability under different nutritional conditions. Interestingly, we found EPSPS as a vulnerable target only when grown on 7H9 medium. When supplemented with aromatic amino acids (7H9 + L-tryptophan + L-phenylalanine + L-tyrosine) or grown on a rich medium (LB), we observed normal bacterial growth of CRISPRi-inactivated *aroA* gene.

MATERIALS AND METHODS

Bacterial Strains, Growth Conditions and Transformation.

Escherichia coli DH10B strain was used for all cloning procedures and routinely grown in LB medium (broth and agar), at 37°C. *Mycobacterium smegmatis* mc²155 strain [19] was kindly provided by Dr. William R. Jacobs, Jr., Albert Einstein College of Medicine, NY, USA. *M. smegmatis* was used for gene knockout and knockdown experiments, and it was grown in LB medium, Difco™ Middlebrook 7H9 broth (Becton Dickinson – BD), supplemented with 0.05% (v/v)

Tween 80 (Sigma-Aldrich), and 0.2% (v/v) glycerol (MERCK), or Difco™ Middlebrook 7H10 Agar (BD), supplemented with 0.5% (v/v) glycerol. Wherever required, the following antibiotics or small molecules were used: 50 µg/mL ampicillin (Amp - Sigma-Aldrich), 25 µg/mL kanamycin (Kan - Sigma-Aldrich) for culturing recombinant *E. coli* strains. Also, 25 µg/mL Kan, 50 µg/mL hygromycin (Hyg – Invitrogen), 100 ng/mL anhydrotetracycline (ATC – Sigma-Aldrich), 50 µg/mL of each amino acids L-tryptophan (FisherBiotech), L-phenylalanine (Sigma-Aldrich) and L-tyrosine (Sigma-Aldrich) for culturing *M. smegmatis* strains. All *E. coli* strains were routinely transformed by electroporation using cuvettes of 0.2 cm, with a 200 Ω resistance, 25 µF capacitance, pulse of 2.25 kV for 3 seconds. On the other hand, for *M. smegmatis* strains, the resistance was changed to 1000 Ω and the pulse to 2.5 kV also for 3 seconds [20]. All primers used in this study are listed in Table 1.

Construction of vectors for recombinant protein expression

The WT *aroA* gene (MSMEG_1890), predicted to code for a 5-enolpyruvylshikimate-3-phosphate synthase (EPSPS), was amplified by PCR using aroA_WT_Primer F and aroA_WT_Primer R (Table 1), 25 ng of genomic DNA of *M. smegmatis* and 10% of DMSO. Genomic DNA was extracted and purified according to a published protocol [21]. The PCR product of 1,354 bp was gel purified, cloned into the pCR™-Blunt (ThermoFisher) vector, and subcloned into the pET-23a(+) (Novagen) expression vector, using NdeI and HindIII restriction sites. Besides, the pET-23a(+)::*aroA*(WT) recombinant vector was used as template for mutagenesis reactions. Four different mutations (D61A,

D61W, R134A and E321N) were incorporated into the gene sequence using the QuickChange XL site-directed mutagenesis kit (Stratagene), along with a set of several primers: primers F and R of aroA_D61A, aroA_D61W, aroA_R134A and aroA_E321N (Table 1). Recombinant clones were confirmed by DNA sequencing.

Construction of the gene knockout (KO) vector

The genomic flanking sequences of *aroA* gene from *M. smegmatis* were PCR-amplified to serve as allelic exchange substrates (AESs) for gene KO. The upstream flanking sequence (1,066 bp), named AES_Up, included 164 bp of the 5'-end of a*roA*, and it was amplified using AES_Up_Primer F and AES_Up_Primer R (Table 1), containing SacI/SpeI and KpnI restriction sites, respectively. The downstream flanking sequence (1,043 bp), named AES_Dw, included 109 bp of the 3'-end of *aroA*, and it was amplified using AES_Dw_Primer F and AES_Dw_Primer R, containing KpnI, and SpeI/HindIII, respectively (Table 1). The AES_Up sequence was cloned into the pUC19 vector, using restriction sites for SacI and KpnI, followed by the AES_Dw insertion using KpnI and HindIII restriction sites. Both AES sequences were confirmed by DNA sequencing. Next, the vector was digested with KpnI, the cohesive endings were filled with *Pfu* DNA polymerase (QuatroG P&D), and the resulting vector was dephosphorylated by CIP (Invitrogen). Then, a 1.2 kb kanamycin resistance cassette from the pUC4K vector was ligated between the AESs. Finally, the whole construction was cut out from pUC19 with SpeI, and inserted into the SpeI site of pPR27xylE vector [22], to yield plasmid pPR27::KO_aroA (Table 1), used to perform allelic replacement.

Construction of gene complementation (CO) vectors

The wild-type (WT) and the four mutant *aroA* sequences (D61A, D61W, R134A and E321N) were transferred from pET-23a(+) vector to the pMVHG1 shuttle vector [23], using the NdeI and HindIII restriction sites. Each gene sequence (WT and mutants) was ligated downstream to the heat shock promoter P_{hsp60}. Then, the P_{hsp60}::*aroA* sequences were cut out with XbaI, gel-purified, and inserted into the XbaI-dephosphorylated site of the pNIP40/b plasmid, yielding five different rescue plasmids (Table 1).

Construction of gene knockdown (KD) vectors

The vulnerability of *aroA* gene was evaluated using the CRISPRi system, developed by Rock and colleagues [18]. The PLJR962 vector backbone was linearized by BsmBI digestion and gel-purified. Three small-guide RNAs (sgRNAs) scaffolds were built to target different regions of the *aroA* coding sequence (Fig. 1). They were designed to bind the non-template (NT) strand of *aroA* gene, in regions where three different PAM (protospacer adjacent motif) sequences (Table 1) were identified using an in-house script written in Python and made publicly available in the GitHub repository (https://github.com/Eduardo-vsouza/sgRNA_predictor). A sgRNA targeting the *mmpL3* (MSMEG_0250) gene was used as a positive control of knockdown experiments.

Two partially complementary oligonucleotides (20-25-nt in length) were designed for each sgRNA scaffold (PAM1, PAM2 and PAM3 primers F and R -

Table 1). The first nucleotide of each sgRNA started with an “A” or “G” to ensure high transcription efficiency. After annealing (95°C for 5 min; decrease 0.1°C/sec until reaching 25°C), oligos retain single-strand 5’-ends that are complementary to the cohesive ends of BsmBI-digested CRISPRi vector. The ligation of sgRNA scaffolds into the vector backbone using T4 DNA ligase (23°C for 16 h) was confirmed by BsmBI digestion and DNA sequencing.

Knockout of the *aroA* gene from *M. smegmatis* and gene complementation

The strategy used for gene knockout experiments was based on a published protocol [24]. First, all rescue plasmids (100-300 ng) were introduced into thawed electrocompetent *M. smegmatis* cells (200 µL) by electroporaton, including a control empty vector (pNIP40::Ø), and selected for their hygromycin resistance (Hyg^R) at 37°C. After three incubation days, one isolated colony of each transformation was grown in 5 mL of LB medium, and electrocompetent cells were prepared again. Then, the pPR27::KO_*aroA* vector was introduced into each merodiploid strain, and transformants were selected on solid LB + kanamycin + hygromycin, at 32°C (permissive temperature), for their kanamycin resistance (Kan^R), and for the presence of the *xylE* reporter gene ($xylE^+$) with the addition of a drop of 1% catechol solution (Sigma-Aldrich). Three yellow colonies (Kan^R, Hyg^R, $XylE^+$) were grown in liquid LB, with kanamycin and hygromycin, at 32°C and 180 rpm, until reaching an optical density (OD) of 0.6-1.0 at 600 nm. Approximately 1 x 10^7 CFUs were then plated on solid LB + kanamycin + hygromycin + 2% sucrose counter-selective plates, in triplicate, and incubated at 39°C for five days. The inoculum was determined by plating each culture on the

same medium, but in the absence of sucrose, at the permissive temperature (32°C), for seven days. Plates were analyzed for the presence of recombinant white colonies (Kan^R, Hyg^R, $XylE^-$, Suc^R) with a drop of catechol. Where possible, white colonies were selected to have their genomic DNA extracted to unambiguously confirm the allelic exchange event in the *aroA* locus by PCR. Amplification reactions were performed with DCO_Primer F and DCO_Primer R (Table 1). DCO_Primer F anneals upstream from *aroA* locus, outside the recombination region, while DCO_Primer R anneals inside the kanamycin resistance cassette (Fig. 2A). An amplicon of 1,813 bp in length was obtained from allelic exchange mutants that underwent a double crossover event (Fig. 2B). The WT genomic DNA of WT *M. smegmatis* was used as a negative control. The same experiment was performed in 7H9 and 7H10 broths for comparison purposes.

Aerobic growth curves of complemented strains

The complemented strains that were viable after the deletion of the wild-type *aroA* chromosomal copy were grown in LB medium + kanamycin + hygromycin, until reaching the early-log phase (OD_{600} ≈0.2). Then, cultures were diluted into fresh LB medium with antibiotics to a theoretical OD_{600} of 0.02, and divided (16 mL) in three conical tubes of 50 mL. Cultures were further incubated for 12 hours, at 37°C, under shaking (180 rpm) and aerobic conditions. Aliquots of 1 mL were taken every 3 hours and OD_{600} was measured. Results were expressed as mean ± standard deviation (SD) of three biological replicates.

Gene knockdown by CRISPRi

Knockdown experiments using CRISPRi were performed on liquid and solid media. First, electrocompetent *M. smegmatis* cells were transformed with PLJR962 constructions containing the sgRNA scaffold coding sequences (see section “Construction of gene knockdown (KD) vectors”), and transformants were selected on solid LB with kanamycin. After three days of incubation, three isolated colonies were cultivated in 5 mL of LB for 48 h, at 37°C, under shaking (180 rpm). Next, cultures were diluted (1:200) in LB (100 mL) containing kanamycin, and further incubated to reach an OD_{600} of 0.2 (for growth curve) or 0.6 (for drop method on plates). For gene KD in liquid medium, cultures were further diluted in fresh medium (OD_{600} ≈0.02) containing kanamycin, equally divided (16 mL) in three conical tubes of 50 mL, with or without ATC, and grown for 24 h at 37°C. Samples (1 mL) were taken every 3 h. Results were expressed as mean ± standard deviation (SD) of three biological replicates. For gene KD in solid medium, drops of 5 µL were plated on solid LB containing kanamycin, with or without ATC. The first spot contained approximately 5,000 cells, and the other three subsequent spots were tenfold serially diluted. Plates were incubated for 3-4 days at 37°C. A negative (PLJR962::Ø) and a positive control (PLJR962::*mmpL3*) were employed for each condition. Additionally, KD experiments were performed in 7H9/7H10 media in the presence, or absence of aromatic amino acids.

Protein Extraction of *M. smegmatis*

For each sample of gene KD in liquid medium, total protein was extracted in 0h and 18h, as previously described [25, 26]. Cellular pellets were washed twice with 10 mM Tris-HCl pH 8.0 and then collected by centrifugation (4,000 rpm, 15 min, 4°C) (Hitachi himac CR21G centrifuge) and resuspended in 2 mL of the same buffer. Cells were disrupted by sonication (10 pulses of 10 s, with intervals of 1 min on ice at 21% of amplitude) using the Sonics Vibra Cell equipment (High Intensity Ultrasonic Processor, 750 Watt model) with a 13 mm probe, centrifuged (13,000 rpm, 30 min, 4°C) and the supernatant (soluble proteins) was stored at -80°C.

Western Blots

Anti-*M. tuberculosis* EPSPS (*Mt*EPSPS) mouse polyclonal antibody was produced immunizing a mouse with 50 µg of purified recombinant *Mt*EPSPS containing Freund's incomplete adjuvant (Sigma-Aldrich, USA) (total volume of 100 µL) by subcutaneous route, followed by a booster injection after one month. The mouse was euthanized by deep isoflurane inhalation one month later, and blood was collected by the descendant aorta. Serum was separated by centrifugation at 10,000 x g for 10 min, aliquoted, and stored at -80°C [26]. The western blot was performed in triplicate. Approximately 30 µg of *M. smegmatis* proteins from detergent fraction were boiled at 70°C for 10 min, loaded on 12% sodium dodecyl sulfate polyacrylamide gels (SDS-PAGE), and transferred to nitrocellulose membranes (Merck Millipore, Ltd-Ireland) in Buffer Tris 25 mM, glycine 192 mM pH 8.8 and methanol 20% for 4h at 70 v. After transfer, the membrane was blocked with 5% non-fat dried milk (Santa Cruz Biotechnology,

USA), 0.05% tween-20 (Sigma-Aldrich, USA) in TBS (T-TBS) (2h, 4°C) and probed with anti-*Mt*EPSPS polyclonal mouse antibody in a 1:500 dilution (overnight at 4°C). Membranes were washed three times with T-TBS, and alkaline phosphatase-conjugated anti-mouse secondary antibody (Invitrogen, USA) was used at a dilution of 1:5,000 [27]. Chemiluminescent substrate (Novex by Life Technologies, USA) was used for detection with ChemiDoc (Bio-Rad, USA).

Overexpression of WT and mutants of *M. smegmatis*

E. coli cells were transformed with recombinant pET-23a(+) plasmids carrying the WT or mutants (R134A, E321N or D61W) of *aroA* gene, and selected on solid LB with ampicillin. A single colony was grown in LB medium (5 mL) with antibiotic, at 37°C, O/N. Pre-cultivated inocula were then diluted (1:1000) in fresh LB (for WT, R134A and E321N) or Terrific Broth (TB) media (for D61W), containing ampicillin. After reaching an OD_{600} of 0.4-0.6, cultures were grown for 23 h at 37°C, under shaking (180 rpm) and aerobic conditions. Protein expression was achieved without isopropyl β-D-1-thiogalactoside (IPTG) induction. Cells were harvested by centrifugation (11,800 x g for 30 min, at 4°C), and stored at -20°C. As a negative control of the expression, the same procedure was employed for *E. coli* cells carrying pET-23a(+) without the *aroA* gene (pET23a(+)::Ø). The expression of soluble proteins was confirmed by 12% SDS-PAGE stained with Coomassie Brilliant Blue.

Purification of recombinant proteins by liquid chromatography

Recombinant WT and mutant proteins were purified using two or three chromatographic steps. All purification steps were carried out in an ÄKTA system (GE Healthcare® Life Sciences) at 4°C. Approximately 3.2 g of cells overproducing each protein were collected. Cells were suspended in 25 mL of 50 mM Tris–HCl pH 7.8 (buffer A), and incubated for 30 min in the presence of 0.2 mg/mL lysozyme (Sigma-Aldrich), under slow stirring. Cells were disrupted by sonication (4 pulses of 20 s, with intervals of 1 min on ice, at 60% of amplitude). Cell debris were removed by centrifugation (11,800 x g for 60 min, at 4 °C). The supernatant was incubated with 1% (w/v) of streptomycin sulphate (Sigma-Aldrich) for 30 min at 4°C, under gently stirring, and centrifuged. The supernatant was dialyzed twice against 2 L of buffer A, using a dialysis tubing with a cutoff filter of 12–14 kDa. The samples were clarified by centrifugation and loaded onto a Q-Sepharose Fast Flow (GE Healthcare® Life Sciences) column, pre-equilibrated with buffer A. Adsorbed proteins were eluted by a 20 column volume (CV) linear gradient (0 - 100%) of 50 mM Tris–HCl NaCl 1M pH 7.8 (buffer B), at 1 mL/min flow rate. Protein elution was monitored by UV detection at 215, 254, and 280 nm. Eluted fractions containing the protein of interest were pooled and ammonium sulphate was added to a final concentration of 1 M. After an incubation period of 30 min at 4°C, and subsequent centrifugation, the supernatant was loaded on a HiLoad 16/10 Phenyl Sepharose HP (GE Healthcare® Life Sciences) column, pre-equilibrated with 50 mM Tris-HCl $(NH_4)_2SO_4$ 1 M pH 7.8 (buffer C). Proteins were eluted by a 20 CV linear gradient (100 - 0% ammonium sulphate) in buffer A, at 1 mL/min flow rate. For WT and R134A mutant, a Mono Q HR 16/10 (GE Healthcare® Life Sciences) column was used as a third step. Protein fractions eluted from the second column were

pooled, centrifuged and loaded into the last column, pre-equilibrated with buffer A. Proteins were eluted by a 15 CV linear gradient in buffer B (0 - 100%), at 2 mL/min flow rate, pooled and dialyzed against buffer A, and finally stored at -80°C. All protein fractions were analyzed by 12% SDS-PAGE stained with Coomassie Brilliant Blue. Protein homogeneity above 95% was checked by densitometry in a GelDoc (Bio-Rad) equipment. Protein concentration was determined by BCA method (Thermo Scientific Pierce™ BCA protein Assay Kit).

Protein identification by LC-MS/MS

Recombinant *Ms*EPSPS enzymes were precipitated with chloroform/methanol [28]. Pellets were resuspended in 100 mM Tris-HCl pH 7.0 containing 8 M urea (Affymetrix USB) and disulfide bonds were reduced in 5 mM dithiothreitol (DTT) (Ludwig Biotec) for 20 min at 37°C. After that, cysteine residues were alkylated with 25 mM iodoacetamide (IAM) (Sigma-Aldrich) for 20 min at room temperature in the dark. Urea was diluted to 2 M with 100 mM Tris-HCl pH 7.0 and trypsin (Promega) was added at a mass ratio of 1:100 (trypsin:protein). Digestion was incubated overnight at 37°C. Formic acid (Merck) was added to end the reaction (5% v/v, final concentration). Tryptic peptides were then separated in a reversed phase C18 (5 µm ODS-AQ C18, Yamamura Chemical Lab) column using a nanoUPLC (nanoLC Ultra 1D plus, Eksigent, USA) and eluted (400 nL/min) with acetonitrile gradient (5%-80%) (LiChrosolv®, Merck) with 0.1% formic acid. Eluting peptide fragments were ionized by electrospray ionization and analyzed on a LTQ-XL Orbitrap Discovery hybrid instrument (Thermo Fisher Scientific). The LC–MS/MS procedure was performed according to the data-dependent acquisition (DDA) method. Precursors were collected from

400-1600 m/z at 30,000 resolution in the Orbitrap and the eight most abundant ions per scan were selected to collision-induced dissociation (CID), using helium as the collision gas, in the ion trap. Raw files were searched in the PatternLab for Proteomics platform [29] with a database containing forward and reverse *E. coli* BL21-DE3 reference proteome and *Ms*EPSPS WT and mutants sequences using Comet [30]. Carbamidomethyl was set as a fixed modification. Search results were filtered to a false discovery rate of 1% through the module Search Engine Processor from PatternLab for Proteomics.

EPSPS enzyme activity assays

Recombinant *Ms*EPSPS enzymes were assayed in the forward direction, using a continuous spectrophotometric rate assay [31, 32]. Enzyme activity was measured in a coupled assay with purine nucleoside phosphorylase from *M. tuberculosis* (*Mt*PNP; EC 2.4.2.1), and 2-amino-6-mercapto-7-methylpurine ribonucleoside (MESG), which was synthesized according to a published protocol [33] (Supplemental Material - Fig. S1)**.** All activity assays were performed in 100 mM Tris–HCl buffer, pH 7.8, at 25°C for 3 min, using 138 nM of *Mt*PNP and 1.7 nM of *Ms*EPSPS. Apparent steady-state kinetic constants were determined by monitoring the WT and mutant EPSPS activities at varying concentrations of 2-phosphoenolpyruvate (PEP – Sigma-Aldrich), and fixed-saturating concentrations of shikimate-3-phosphate (S3P - Sigma-Aldrich) (Supplemental Material – Table S1). All measurements were performed in a 1.0 cm path length quartz cuvette, in duplicate, and the rate of inorganic phosphate (Pi) production was measured in a UV/Vis spectrophotometer (Shimadzu). Steady-state kinetic

406 constants were obtained by non-linear regression analysis of the kinetic data
407 fitted to the Michaelis-Menten equation ($v = V_{max}$ x [S]/(K_m + [S])) using the
408 SigmaPlot 14.0 software (SPSS, Inc). The k_{cat} values were calculated using the
409 following k_{cat} equation ($k_{cat} = V_{max}$/[E]t).

410

411 **RESULTS**

412 ***In vitro* essentiality of *aroA* gene from *M. smegmatis***

413 We knocked out the *aroA* gene from *M. smegmatis* to evaluate its
414 essentiality *in vitro.* First, a set of merodiploid strains, holding an extra copy of the
415 WT or mutants *aroA* genes (D61A, D61W, E321N, and R134A), received a
416 plasmid carrying the allelic exchange substrate (pPR27::KO_*aroA*), which was
417 confirmed by the presence of bright yellow colonies after catechol addition (see
418 Methods, section "Knockout of the aroA gene from *M. smegmatis* and gene
419 complementation"). Only three independent yellow colonies were grown under
420 permissive conditions, and then submitted to counterselective pressures (growth
421 temperature of 39°C and 2% sucrose) on solid LB medium. From an inoculum of
422 ≈10^7 CFUs per plate, several white colonies (Kan^R, Hyg^R, $XylE^-$, Suc^R), holding
423 the WT *aroA* extra copy, were obtained. Only three colonies were observed from
424 the strain carrying no extra copy of *aroA* (pNIP::Ø), but they revealed to be yellow
425 after catechol testing (Kan^R, Hyg^R, $XylE^+$, Suc^R). This result suggests that in the
426 absence of a functional copy of the *aroA* gene the mycobacteria is unable to
427 survive, confirming the essentiality of this gene *in vitro*. The same result was
428 observed in 7H10 medium.

We conducted similar experiments with merodiploid strains containing an extra copy of *aroA* gene (WT, D61A, D61W, R134A and E321N). In both LB and 7H10 media, only the WT strain and strains carrying mutations in the aspartic acid residue (D61A and D61W) survived the allelic exchange event. To confirm the DCO event, a PCR reaction was carried out using genomic DNA extracted from each of the white colonies obtained (Fig. 2B).

Mutations in the Asp61 residue of *Ms*EPSPS enzyme enables mycobacterial growth

Growth curves were performed to evaluate the impact of mutations in the aspartic acid 61 residue (D61A or D61W) of *Ms*EPSPS on bacilli grown in LB medium. We found no differences in the growth of D61 mutants, when compared to control strains (Fig. 2C). This suggests that the replacement of this hydrophilic amino acid by the hydrophobic alanine or tryptophan residues does not abolish the *Ms*EPSPS activity inside cells.

Expression, purification and identification of recombinant *Ms*EPSPSs

The overexpression of recombinant *Ms*EPSPS proteins (WT, D61W, R134A and E321N) in the soluble fraction was confirmed by SDS-PAGE, with an apparent molecular mass of 46 kDa. Homogeneous preparations were obtained using a 3-step protocol for both *Ms*EPSPS WT and D61W, whereas a 2-step protocol was employed for mutants R134A and E321N (Table 2, Supplemental Material – Fig. S2). Recombinant *Ms*EPSPS WT, D61W, E321N and R134A

mutants were submitted to trypsin digestion and peptides were analyzed by LC-MS/MS. A coverage of approximately 90% was obtained for each protein with 85, 97, 80 and 74 unique peptides identified, respectively. Furthermore, it was possible to identify and validate all point mutations (Supplemental Material - Fig. S3-5).

Kinetic parameters of WT and mutant EPSPS enzymes

EPSPS enzymes are known to catalyze the transfer of the carboxyvinyl portion of the phosphoenolpyruvate substrate (PEP) to the carbon-5 hydroxyl group of shikimate-3-phosphate (S3P), forming the enolpyruvylshikimate-3-phosphate (EPSP) product and releasing inorganic phosphate (Pi). To determine the kinetic parameters of WT and mutant enzymes, we performed a coupled assay using *Mt*PNP and MESG. The dependence of initial velocity on PEP as a variable substrate at fixed-saturating S3P concentration (see Supplemental Material – Table S1) followed hyperbolic Michaelis-Menten kinetics. The apparent steady-state kinetic parameters for WT and mutant *Ms*EPSPS enzymes are presented in Table 3.

aroA silencing with CRISPRi in *M. smegmatis*

The vulnerability of *aroA* from *M. smegmatis* was assessed by using CRISPRi in different growth contexts. Using an in-house script written in Python, twelve targets were found in the non-template strand (NT) of *aroA* coding sequence. Three distinct sequences next to functional PAMs (5'-NAGCAT-3', 5'-NNAGGAT-3', and 5'-NNAGCAG-3') and located at the first half of the gene (Fig.

1) were chosen to be targeted by three sgRNAs (named PAM1, PAM2, and PAM3). The vulnerability of this gene was evaluated in both rich media (solid and liquid LB – Fig. 3A-D) and defined media (solid 7H10 and liquid 7H9 – Fig. 3E-H) in the presence or absence of ATC 100 ng/mL, using the vulnerable *mmpL3* gene as positive control. We did not observe any difference in growth in the presence or absence of ATC in both solid and liquid rich media (Fig. 3B-D). In contrast, with all target sequences tested (adjacent to PAM 1 to 3) in solid and liquid defined media, we observed a decrease in bacterial growth from 15h in the presence of ATC, indicating that *aroA* gene silencing leads to a bacterial growth perturbation in poor nutrients media (Fig. 3F-H).

Next, we supplemented solid defined medium (7H10) with aromatic amino acids (L-tryptophan + L-phenylalanine + L-tyrosine), which are end products of the Shikimate pathway (Fig. 4A), and repeated the *aroA* knockdown using the CRISPRi system. Interestingly, we did not observe any difference in growth in the presence or in the absence of ATC (Fig. 4B-D).

DISCUSSION

Target validation is a required part of any effort to develop new chemotherapeutic agents based on rational-drug design. Essentiality for growth and/or survival is a critical feature of a target, as the chemical inhibition of non-essential gene products are not expected to kill the infective agent and hence to achieve the desired therapeutic outcome. Here, by performing an allelic exchange-based gene knockout experiment, we show that the *aroA*-encoded EPSPS gene product is essential for *M. smegmatis* growth *in vitro* (Fig. 2). This

agrees with previous reports based on transposon-mediated mutagenesis that the orthologous gene from *M. tuberculosis* is also essential [34].

Previously, the *aroK* gene from *M. tuberculosis*, which encodes shikimate kinase (*Mt*SK), was also found to be essential [13]. Interestingly, the supplementation of neither the end product of the pathway, chorismate, nor aromatic amino acids (tyrosine, tryptophan and phenylalanine) was sufficient to allow growth of *aroK* mutants. It was suggested that *Mt*SK, like *aroK*-encoded SK from *Escherichia coli* [35], could have other functions unrelated to the shikimate kinase activity [13]. We thus evaluated whether the EPSPS activity of *aroA* protein product is responsible for *aroA* gene essentiality. To do so, we constructed four merodiploid strains containing extra copies of *aroA* encoding point mutants of EPSPS (D61A, D61W, R134A and E321N).

The selection of these residues was based on a previous experimental work on EPSPS from *E. coli* (*Ec*EPSPS) [36] and on computational studies of EPSPS from *M. tuberculosis* (*Mt*EPSPS) [37]. It was already demonstrated that a mutation in the aspartic acid-49 (D49) residue to an alanine leads to a reduction of 24,000 times in the specific activity of the enzyme from *E. coli*. The reasons for that are still unclear, but the authors hypothesized an indirect effect on the lysine-22 (K22) residue, which is known to participate directly in catalysis. On the other hand, the residues arginine-124 (R124) and aspartic acid-313 (D313), which are near to the PEP binding site, are directly involved in the catalytic reaction. When those residues were mutated to an alanine and glutamic acid, respectively, the enzymes had their catalytic activity reduced to around 5,000 and 20,000 times, showing that residues R124 and D313 are critical to the correct function of the *Ec*EPSPS enzyme [36]. In addition, *in silico* predictions using the enzyme of *M.*

525 *tuberculosis* suggested that changing the aspartic acid-54 (D54) residue (which
526 corresponds to D49 in *Ec*EPSPS and D61 in *Ms*EPSPS enzymes) to an alanine
527 (D54A) or tryptophan (D54W) should cause a significant impact on the protein
528 stability and, consequently, a negative impact on the enzyme's activity [37].

529 To confirm the expected impact of these point mutations on *Ms*EPSPS
530 activity, we cloned, expressed and purified mutants D61W, R134A and E321N.
531 The kinetic properties of the wild-type recombinant enzyme (WT) and three
532 mutants were measured and compared (Table 3). The K_m for the substrate PEP
533 in mutant forms of *Ms*EPSPS increased from 11.5 up to 42 times when compared
534 to WT enzyme. These results suggest an increased overall dissociation constant
535 for PEP substrate binding to mutant proteins at fixed-saturating concentrations of
536 S3P. The impact on enzyme turnover (k_{cat}) ranged from 1.2-fold (E321N) to 5.1-
537 fold (D61W) decrease (Table 3). Accordingly, more pronounced effects on the
538 catalytic efficiencies (k_{cat}/K_m) of mutants were observed. We found a reduction of
539 44- (E321N), 59- (D61W) and 125-fold (R134A) in k_{cat}/K_m for these enzymes.
540 These reductions in the apparent second-order rate constants suggest lower
541 association rate constants for PEP substrate binding to *Ms*EPSPS enzyme.
542 Therefore, we can conclude that mutations in these specific residues affect
543 directly the catalytic efficiency of the *Ms*EPSPS, although to a lesser extent than
544 expected, based on previous studies with orthologs [36].

545 In the intracellular environment, however, the impact of each mutation in
546 the cell metabolism was different. The replacement of aspartate-61 with
547 hydrophobic residues (alanine or tryptophan) was not lethal (Fig. 2B) and did not
548 impart in any growth defect of *M. smegmatis* (Fig. 2C). This may suggest that
549 inside cells aspartate-61 is dispensable for *Ms*EPSPS activity, or the 59-fold

550 decrease in the k_{cat}/K_m value for the PEP substrate is not sufficient to impair cell
551 growth. On the other hand, we were not able to retrieve viable colonies after
552 knocking out the WT *aroA* gene from merodiploid strains containing an extra copy
553 of *aroA* gene encoding *Ms*EPSPS R134A or E321N mutants. These results
554 suggest that both mutations are lethal under the conditions tested and
555 corroborate the proposition that *aroA* essentiality is causally linked to EPSPS
556 activity. As pointed out by some of us, establishing a causal link between gene
557 essentiality and the biological function of its protein product under scrutiny should
558 be an indispensable step in target validation for drug development [24]. This view
559 is reinforced by the growing number of proteins found to exhibit multiple and
560 unrelated tasks, the so-called moonlighting proteins [38].

561 Next, we addressed the issue of target vulnerability. A target should not
562 only be essential but also vulnerable, otherwise chances are low to develop
563 bioactive compounds that effectively kill or impart growth defects on infective
564 agents. To evaluate *Ms*EPSPS vulnerability, we performed gene knockdown
565 experiments using the CRISPRi system developed for mycobacteria [18]. Using
566 an in-house Python script, we selected target sequences adjacent to PAM motifs
567 whose repression strengths were characterized previously [18]. The experiments
568 were conducted in both rich (LB, Fig. 3A-D) and defined (7H9 or 7H10, Fig. 3E-
569 H) media, with markedly different results. As expected, the sgRNA control
570 targeting the *mmpL3* gene was found to be vulnerable in both nutritional
571 conditions, either in liquid or solid media. Silencing *mmpL3* caused a cessation
572 of bacterial growth by 15 h, and using the drop method on plates, it was observed
573 a reduction of at least 1000-fold in the CFU counting (Fig. 3A and 3E). This gene
574 codes for the mycobacterial membrane MmpL3 protein, which is responsible for

trehalose monomycolate transportation through the cell inner membrane [39]. In *M. tuberculosis* and *M. smegmatis*, it was shown that silencing *mmpL3* expression disrupts bacterial growth [18,40], leading to accumulation of TDM and cell death [41]. Differently from MmpL3, *Ms*EPSPS was found to be vulnerable only in defined media and in the presence of ATC, irrespective of PAM's repression strength. Silencing *aroA* gene caused an impairment of the bacterial growth after 18 h, but not a complete cessation (Fig. 3F-H). This suggests that the suppression of *Ms*EPSPS expression observed (Supplemental Material – Fig. S6-7) does not cause bacterial killing, but rather, growth impairment (Fig. 3F-H). Moreover, supplementation with aromatic amino acids (L-phenylalanine, L-tyrosine and L-tryptophan) is sufficient to rescue the growth impairment of *aroA*-silenced strain (Fig. 4B-D).

Drawing a parallel between our results of *aroA* gene knockout and *aroA* gene knockdown with CRISPRi, it is evident that both experimental approaches serve to understand different biological phenomena. By performing gene knockout and complementation experiments, we found that *aroA* gene of *M. smegmatis* is essential regardless of the nutritional context (Fig. 2A-C, Fig. S8). This is an evidence that this bacterium is unable to grow in the complete absence of *Ms*EPSPS, most likely because of its incapacity of producing chorismate [13]. This metabolite is a precursor for the synthesis of folates, aromatic amino acids, ubiquinones, naphtoquinones, menaquinones and mycobactins (Fig. 4A), being indispensable for bacterial metabolism. On the other hand, even after resulting in markedly reduced levels of *Ms*EPSPS (Fig. S6 and S7), *aroA* gene knockdown using the CRISPRi system impaired bacterial growth only in a poor nutritional context (Fig. 3), and supplementation of aromatic amino acids was sufficient to

restore normal growth (Fig. 4B-D). Presumably, very low levels of *Ms*EPSPS can support the operation of the shikimate pathway to the level required to produce most of the metabolic end products that have chorismate as a precursor compound, except for the aromatic amino acids. The implications of our results are twofold. By growing *aroA*-knocked down bacteria in different nutritional conditions, rich medium, defined medium and defined medium with supplementation, we were able to characterize *Ms*EPSPS vulnerability in more detail. In a context of low availability of aromatic amino acids, *Ms*EPSPS can be considered a vulnerable target. Otherwise, under the presence of appropriate levels of L-phenylalanine, L-tyrosine and L-tryptophan, our experiments suggest *Ms*EPSPS would not be a vulnerable target, as the incomplete inhibition of its activity by antimicrobial agents is not expected to abrogate the synthesis of the other chorismate-dependent end products and lead to growth impairment and cell death. Moreover, the results we obtained using both gene knockout and gene knockdown approaches raises a cautionary note to the use of gene knockdown experiments to infer gene essentiality. As was the case with *Ms*EPSPS, the presence of very low protein levels, undetectable by means of Western Blot assays (Figs. S6 and S7), can lead to a completely different phenotype when compared to that obtained under the complete absence of the same protein, as in knocked out strains (Figs. 2A-C and S8), and consequently to a misappreciation of gene essentiality.

Acknowledgments:

We thank Sara Fortune and Jeremy Rock for providing the pLJR962 plasmid and Hector Morbidoni and Luis Saraiva Timmers for insightful discussions. C.V.B., P.M. and L.A.B. would like to acknowledge financial support given by CNPq/FAPERGS/CAPES/BNDES to the National Institute of Science and Technology on Tuberculosis (INCT-TB), Brazil (grant numbers: 421703-2017-2/17-1265-8/14.2.0914.1). C.V.B. (310344/2016-6), P.M. (305203/2018-5) and L.A.B. (520182/99-5) are research career awardees of the National Council for Scientific and Technological Development of Brazil (CNPq). This study was financed in part by the Coordenação de Aperfeiçoamento de Pessoal de Nível Superior—Brasil (CAPES)—Finance Code 001.

Conflicts of Interest:

The authors declare no conflict of interest.

References

[1] WHO. (2019). GLOBAL TUBERCULOSIS REPORT 2019. Retrieved from http://apps.who.int/bookorders.

[2] Tiemersma, E.W., van der Werf M.J., Borgdorff M.W., Williams B.G., & Nagelkerke N.J. (2011). Natural history of tuberculosis: duration and fatality of untreated pulmonary tuberculosis in HIV negative patients: a systematic review. *PLoS One*. 6(4):e17601. Published 2011 Apr 4. doi:10.1371/journal.pone.0017601.

[3] Schatz, A., & Waksman, S.A. (1944). Effect of Streptomycin and Other Antibiotic Substances upon *Mycobacterium tuberculosis* and Related Organisms. *Proceedings of the Society for Experimental Biology and Medicine*, 57(2), 244–248. https://doi.org/10.3181/00379727-57-14769

[4] Boritsch, E.V.A.C., & Brosch, R. (2016). Evolution of *Mycobacterium tuberculosis*: New Insights into Pathogenicity and Drug Resistance. *Microbiol Spectr*, 4(5), 1–20. https://doi.org/10.1128/microbiolspec.TBTB2-0020-2016

[5] Mabhula, A., & Singh, V. (2019). Drug-resistance in *Mycobacterium tuberculosis*: where we stand. *MedChemComm*, 10(8), 1342-1360.

[6] Nguyen, Q. H., Contamin, L., Nguyen, T. V. A., & Bañuls, A. L. (2018). Insights into the processes that drive the evolution of drug resistance in *Mycobacterium tuberculosis*. *Evolutionary applications*, 11(9), 1498-1511.

[7] Silver, L. L. (2016). Appropriate targets for antibacterial drugs. *Cold Spring Harb Perspect Med*. 6(12), a030239.

[8] Ramachandran, V., Singh, R., Yang, X., Tunduguru, R., Mohapatra, S., Khandelwal, S., & Datta, S. (2013). Genetic and chemical knockdown: A complementary strategy for evaluating an anti-infective target. *Adv Appl Bioinform Chem*, 6(1), 1–13. https://doi.org/10.2147/AABC.S39198

[9] Wei, J. R., Krishnamoorthy, V., Murphy, K., Kim, J. H., Schnappinger, D., Alber, T., & Rubin, E. J. (2011). Depletion of antibiotic targets has widely varying effects on growth. *Proc Natl Acad Sci U S A.*, 108(10), 4176-4181.

[10] Park, Y., Pacitto, A., Bayliss, T., Cleghorn, L. A. T., Wang, Z., Hartman, T., & Boshoff, H. I. (2017). Essential but Not Vulnerable: Indazole Sulfonamides

668 Targeting Inosine Monophosphate Dehydrogenase as Potential Leads against
669 *Mycobacterium tuberculosis*. *ACS Infectious Diseases*, 3(1), 18–33.
670 https://doi.org/10.1021/acsinfecdis.6b00103.

671 [11] Ducati, R. G., Basso, L. a, & Santos, D. S. (2007). Mycobacterial shikimate
672 pathway enzymes as targets for drug design. *Curr Drug Targets*, 8(3), 423–435.
673 https://doi.org/10.2174/138945007780059004.

674 [12] Herrmann, K. M., & Weaver, L. M. (1999). The Shikimate Pathway. *Annu*
675 *Rev Plant Physiol Plant Mol Biol*. 50(1), 473–503.
676 https://doi.org/10.1146/annurev.arplant.50.1.473

677 [13] Parish, T., & Stoker, N. G. (2002). The common aromatic amino acid
678 biosynthesis pathway is essential in *Mycobacterium tuberculosis*. *Microbiology*
679 (Reading, England), 148(Pt 10), 3069–3077. https://doi.org/10.1099/00221287-
680 148-10-3069

681 [14] Rizzi, C., Frazzon, J., Ely, F., Weber, P. G., Da Fonseca, I. O., Gallas, M., &
682 Basso, L. A. (2005). DAHP synthase from *Mycobacterium tuberculosis* H37Rv:
683 Cloning, expression, and purification of functional enzyme. *Protein Expr Purif*,
684 40(1), 23–30. https://doi.org/10.1016/j.pep.2004.06.040

685 [15] Peng, R. H., Tian, Y. S., Xiong, A. S., Zhao, W., Fu, X. Y., Han, H. J., & Yao,
686 Q. H. (2012). A novel 5-enolpyruvylshikimate-3-phosphate synthase from
687 *Rahnella aquatilis* with significantly reduced glyphosate sensitivity. *PloS one*,
688 7(8).

689 [16] Coggins, J. R., Abell, C., Evans, L. B., Frederickson, M., Robinson, D. a,
690 Roszak, a W., & Lapthorn, a P. (2003). Experiences with the shikimate-pathway

691 enzymes as targets for rational drug design. *Biochem Soc Trans*. 31(Pt 3), 548–
692 552. https://doi.org/10.1042/BST0310548

693 [17] McArthur, J. D., West, N. P., Cole, J. N., Jungnitz, H., Guzmán, C. A., Chin,
694 J., & Walker, M. J. (2003). An aromatic amino acid auxotrophic mutant of
695 *Bordetella bronchiseptica* is attenuated and immunogenic in a mouse model of
696 infection. *FEMS Microbiology Letters*, 221(1), 7–16. Retrieved from
697 http://www.ncbi.nlm.nih.gov/pubmed/12694904

698 [18] Rock, J. M., Hopkins, F. F., Chavez, A., Diallo, M., Chase, M. R., Gerrick, E.
699 R., & Fortune, S. M. (2017). Programmable transcriptional repression in
700 mycobacteria using an orthogonal CRISPR interference platform. *Nature*
701 *Microbiology*, 2(February), 1–9. https://doi.org/10.1038/nmicrobiol.2016.274

702 [19] Snapper, S. B., Melton, R. E., Mustafa, S., Kieser, T., & Jr, W. R. J. (1990).
703 Isolation and characterization of efficient plasmid transformation mutants of
704 *Mycobacterium smegmatis*. *Mol Microbiol*. 4(11), 1911–1919.
705 https://doi.org/10.1111/j.1365-2958.1990.tb02040.x

706 [20] Parish, T., & Stoker, N. G. (2015). Mycobacteria Protocols (Third Edit, Vol.
707 101; John M. Walker, ed.). https://doi.org/10.1385/0896034712

708 [21] Kumar, P., Marathe, S., & Bhaskar, S. (2016). Isolation of Genomic DNA
709 from *Mycobacterium* Species. BIO-PROTOCOL, 6(5), 11–14.
710 https://doi.org/10.21769/BioProtoc.1751

711 [22] Pelicic, V., Reyrat, J. M., & Gicquel, B. (1996). Expression of the Bacillus
712 subtilis *sacB* gene confers sucrose sensitivity on mycobacteria. *J Bacteriol*.
713 178(4), 1197–1199. https://doi.org/10.1128/jb.178.4.1197-1199.1996

[23] Pan, F., Jackson, M., Ma, Y., & McNeil, M. (2001). Erratum: Cell wall core galactofuran synthesis is essential for growth of mycobacteria. *J Bacteriol*. 183(23), 6971. https://doi.org/10.1128/JB.183.13.3991

[24] Falcão, V. C. A., Villela, A. D., Rodrigues-Junior, V. S., Pissinate, K., Eichler, P., Pinto, A. F. M., & Bizarro, C. V. (2017). Validation of *Mycobacterium tuberculosis* dihydroneopterin aldolase as a molecular target for anti-tuberculosis drug development. *Biochem Biophys Res Commun*, 485(4), 814–819. https://doi.org/10.1016/j.bbrc.2017.02.137

[25] Trindade, R. V., Pinto, A. F. M., Santos, D. S., & Bizarro, C. V. (2016). Pulse Proteolysis and Precipitation for Target Identification. *J Proteome Res*, 15(7), 2236–2245. https://doi.org/10.1021/acs.jproteome.6b00214

[26] Wink, P. L., Sanchez Quitian, Z. A., Rosado, L. A., Rodrigues, V. D. S., Petersen, G. O., Lorenzini, D. M., Lipinski-Paes, T., Timmers, L. F. S. M., de Souza, O. N., Basso, L.A., & Santos, D. S. (2013). Biochemical characterization of recombinant nucleoside hydrolase from *Mycobacterium tuberculosis* H37Rv. Arch Biochem Biophys, 538(2), 80–94. https://doi.org/10.1016/j.abb.2013.08.011

[27] Villela, A. D., Rodrigues-Junior, V. S., Pinto, A. F. M., Falcão, V. C. de A., Sánchez-Quitian, Z. A., Eichler, P., & Santos, D. S. (2017). Construction of *Mycobacterium tuberculosis* cdd knockout and evaluation of invasion and growth in macrophages. *Mem Inst Oswaldo Cruz*, 112(11), 785–789. https://doi.org/10.1590/0074-02760170105

[28] Wessel, D., & Flügge, U. I. (1984). A method for the quantitative recovery of protein in dilute solution in the presence of detergents and lipids. Anal Biochem, 138(1), 141–143. https://doi.org/10.1016/0003-2697(84)90782-6

738 [29] Carvalho, P. C., Lima, D. B., Leprevost, F. V., Santos, M. D. M., Fischer, J.
739 S. G., Aquino, P. F., & Barbosa, V. C. (2016). Integrated analysis of shotgun
740 proteomic data with PatternLab for proteomics 4.0. *Nat Protoc*, 11(1), 102–117.
741 https://doi.org/10.1038/nprot.2015.133

742 [30] Eng, J. K., Jahan, T. A., & Hoopmann, M. R. (2013). Comet: An open-source
743 MS/MS sequence database search tool. *Proteomics*, 13(1), 22–24.
744 https://doi.org/10.1002/pmic.201200439

745 [31] Webb, M. R. (1992). A continuous spectrophotometric assay for inorganic
746 phosphate and for measuring phosphate release kinetics in biological systems.
747 *Proc Natl Acad Sci U S A*, 89(11), 4884–4887.
748 https://doi.org/10.1073/pnas.89.11.4884.

749 [32] Oliveira, J. S., Mendes, M. A., Palma, M. S., Basso, L. A., & Santos, D. S.
750 (2003). One-step purification of 5-enolpyruvylshikimate-3-phosphate synthase
751 enzyme from *Mycobacterium tuberculosis*. *Protein Expr Purif*, 28(2), 287–292.
752 https://doi.org/10.1016/S1046-5928(02)00708-8

753 [33] Neto, B. A. D., Lapis, A. A. M., Netz, P. A., Spencer, J., Dias, S. L. P.,
754 Tamborim, S. M., Basso, L. A., Santos, D. S., & Dupont, J. (2010). Synthesis and
755 enzymatic evaluation of the guanosine analogue 2-amino-6-mercapto-7-
756 methylpurine ribonucleoside (MESG). Insights into the phosphorolysis reaction
757 mechanism based on the blueprint transition state: SN1 or SN2? *J. Braz. Chem.*
758 *Soc*, 21(1), 151–156. https://doi.org/10.1590/S0103-50532010000100022

759 [34] Griffin, J. E., Gawronski, J. D., DeJesus, M. A., Ioerger, T. R., Akerley, B. J.,
760 & Sassetti, C. M. (2011). High-resolution phenotypic profiling defines genes

761 essential for mycobacterial growth and cholesterol catabolism. *PLoS Pathog*,
762 7(9), 1–9. https://doi.org/10.1371/journal.ppat.1002251

763 [35] Vinella D., Gagny B., Joseleau-Petit D., D'Ari R., & Cashel M. (1996).
764 Mecillinam resistance in *Escherichia coli* is conferred by loss of a second activity
765 of the *AroK* protein. *J Bacteriol*.;178(13):3818–3828.

766 [36] Mizyed, S., Wright, J. E. I., Byczynski, B., & Berti, P. J. (2003). Identification
767 of the catalytic residues of *AroA* (Enolpyruvylshikimate 3-phosphate synthase)
768 using partitioning analysis. *Biochemistry*, 42(23), 6986–6995.
769 https://doi.org/10.1021/bi027217l

770 [37] Timmers, L. F. S. M., Neto, A. M. S., Montalvão, R. W., Basso, L. A., Santos,
771 D. S., & Norberto de Souza, O. (2017). EPSP synthase flexibility is determinant
772 to its function: computational molecular dynamics and metadynamics studies. *J*
773 *Mol Model*. https://doi.org/10.1007/s00894-017-3372-2

774 [38] Chen, C., Zabad, S., Liu, H., Wang, W., & Jeffery, C. (2018). MoonProt 2.0:
775 an expansion and update of the moonlighting proteins database. *Nucleic Acids*
776 *Res*, 46(D1), D640-D644.

777 [39] Fay, A., Czudnochowski, N., Rock, J. M., Johnson, J. R., Krogan, N. J.,
778 Rosenberg, O., & Glickman, M. S. (2019). Two accessory proteins govern
779 MmpL3 mycolic acid transport in mycobacteria. *mBio*, 10(3), e00850-19.

780 [40] McNeil, M. B., & Cook, G. M. (2019). Utilization of CRISPR interference to
781 validate MmpL3 as a drug target in Mycobacterium tuberculosis. *Antimicrob*
782 *Agents Chemother*, 63(8), e00629-19.

783 [41] Degiacomi, G., Benjak, A., Madacki, J., Boldrin, F., Provvedi, R., Palù, G., &
784 Manganelli, R. (2017). Essentiality of mmpL3 and impact of its silencing on
785 Mycobacterium tuberculosis gene expression. *Sci Rep*. 7, 43495.

786

787

788 FIGURE LEGENDS

789 **Figure 1. Knockdown of EPSPS-encoding gene *aroA* in *M. smegmatis* using CRISPR** 790 **interference (CRISPRi). Upper part:** Location of PAM sequences inside *aroA* locus used in this 791 study. From left to right: 5'- NNAGGAT-3', 5'-NNAGCAG-3' and 5'- NNAGCAT-3'. The repression 792 strength of each PAM sequence, according to Rock et al. (2017), is also depicted. **Lower part**: 793 Schematic representation of CRISPRi system associated with *aroA* locus at a target region 794 adjacent to PAM "5'-NNAGCAG-3'". Dead Cas9 (dCas9) is represented in peach color, sgRNA 795 as a single RNA chain in blue with annealing portion in green and paired with the non-template 796 (NT) strand of target DNA. The "5'-AGCAG-3'" from PAM is depicted in red in the template (T) 797 strand of target DNA in 3'-5' orientation.

798 **Figure 2. *aroA* gene from *M. smegmatis* is essential for mycobacterial survival *in vitro*. (A)** 799 Schematic representation of the allelic exchange event in the *aroA* locus. Two putative genes 800 (MSMEG_1891 and MSMEG_1889) flank the *aroA* gene (MSMEG_1890) of *M. smegmatis*. The 801 Allelic Exchange Sequences (AESs) were designed to maintain possible transcriptional and 802 translation regulatory sequences of these two genes. The *aroA* gene was disrupted by the 803 insertion of a kanamycin resistance cassette (1,252 bp), which was also used as a selective 804 marker for homologous recombination. The position of primers used in PCR reactions described 805 in (B) are indicated by black arrows. **(B)** PCR confirming the interruption of the *aroA* gene in 806 merodiploid strains carrying the WT, D61A, or D61W mutant copies. Genomic DNA extracted 807 from white colonies, and a pair of primers specific for the interrupted gene were used for this 808 reaction. A band of 1,813 bp was expected for allelic exchange mutants. Lane M: 1kb plus DNA 809 ladder (Invitrogen). Lane 1: *M. smegmatis* mc²155 genomic DNA (negative control). Lanes 2-8: 810 strains carrying the WT copy of *aroA* gene. Lanes 9-12: strains carrying the D61A (9-10) or D61W 811 (11-12) mutant copies of *aroA* gene. **(C)** Mutations in the Asp61 residue of *Ms*EPSPS does not 812 impair mycobacterial survival and growth *in vitro*. Strains carrying mutations D61A and D61W in 813 the *Ms*EPSPS enzyme were grown for 12 h in LB medium, under aerobic conditions, and aliquots 814 were taken each 3 h for optical density measurement at 600 nm (OD_{600}). Strains carrying the WT 815 *aroA* gene or the empty complementation vector (pNIP::Ø), as well as the reference *M. smegmatis* 816 *mc²155*, were used as growth references. Error bars are standard deviation (SD) of three

817 biological replicates. **(D)** Sequence alignment of EPSPS enzymes from *E. coli* CVM N33429PS 818 (Ec), *M. tuberculosis* H37Rv (Mt) and *M. smegmatis* mc^{2}155 (Ms). Amino acid sequences were 819 aligned by using T-Coffee and Boxshade. The enzyme from *M. smegmatis* shows 53% and 71% 820 of identity with enzymes of *E. coli* and *M. tuberculosis*, respectively. Amino acids indicated by 821 black arrows were chosen for mutagenesis.

822 **Figure 3. Knockdown of *aroA* gene from *M. smegmatis* produces a growth perturbation *in* 823 *vitro.* (A-D)** Growth in rich media (solid and liquid LB). **(E-H)** Growth in defined media (solid 7H10 824 and liquid 7H9). *M. smegmatis* growth curves and dilution spots in the presence or absence of 825 anhydrotetracycline (ATC) (100 ng/mL) for the control gene *mmpL3* **(A and E)** and the *aroA* gene 826 at three different locations adjacent to PAM1, PAM2 and PAM3 **(B-D and F-H)**.

827 **Figure 4. Rescued *M. smegmatis* strains in the presence of the aromatic amino acids. (A)** 828 Schematic representation of shikimate pathway and its end products. **(B-D)** *M. smegmatis* growth 829 in the presence or absence of ATC (100 ng/mL) in solid defined medium (7H10) supplemented 830 with aromatic amino acids (L-phenylalanine, L-tyrosine and L-tryptophan).

831

832

833 **Table 1**. List of oligonucleotides and primers used in this study.

Primers used in the mutation experiments		
	Primer F	**Primer R**
aroA_D61A	TGAGGTCGGTGGCGCGGCTGCGC	GCGCAGCCGCGCCACCGACCTCA
aroA_D61W	GATCATGAGGTCGGTCCAGCGGCTGCGCAGCGC	GCGCTGCGCAGCCGCTGGACCGACCTCATGATC
aroA_R134A	AGCGATGGGCGCTGACCTGGCCTGTTCGTC	GACGAACAGGCCAGGTCAGCGCCCATCGCT
aroA_E321N	CGGTCGGCGCGAGATTACCCACGTCGTGC	GCACGACGTGGGTAATCTCGCGCCGACCG
Primers used for knockout construction		
aroA_WT	TTTCATATGAGTGCACGCGCGGACGA	TTTAAGCTTTCTAGATTCAACGCTGTTGATTCCTCCCC
AES_Up	TTTGAGCTCACTAGTATCGCATCGATGACCGCG	TTTGGTACCCCGCTGATCGTGGAGGTG
AES_De	TTTGGTACCGGGGTCGTCGTCGAGAACAT	TTTAAGCTTACTAGTGAGCGCGCACTCCGGATC
Primers used for amplification of the double crossover		
DCO	AGAAGTCGTGAGTGCCGTCG	GTTTTCCCGGGGATCGCAGT
Oligonucleotides used for sgRNA		
PAM1_NNAGCAT	GGGAGACCTCGACGCCCGCGTCGC	AAACGCGACGCGGGCGTCGAGGTC
PAM2_NNAGGAT	GGGAGCCCTGCGAGGTGGCCAGCGCCG	AAACCGGCGCTGGCCACCTCGCAGGGC
PAM3_NNAGCAG	GGGAACCCCGAGCCGGCGCAGGCCGT	AAACACGGCCTGCGCCGGCTCGGGGT
mmpL3	GGGAGCGACAGATGGCTGCCCTCGTC	AAACGACGAGGGCAGCCAGTCTGTCGC

834

835

836 **Table 2.** Purification yield of recombinant *Ms*EPSPS enzymes.

***Ms*EPSPS Enzymes**[a]	**Column**[b]	**Protein concentration (mg/mL)**	**Eluted volume (mL)**	**Total protein (mg)**	**Yield (%)**	**Homogeneity (%)**
WT	First	13.4	25	334.4	20.7	97.3
	Last	3.6	19		69.4	
D61W	First	6.4	25	160.7	8.5	96.8
	Last	0.7	20		13.7	
R134A	First	20.4	25	510.7	11.2	98.4
	Last	3.0	19		57.1	
E321N	First	13.2	25	330.0	17.3	100
	Last	0.6	96		57.2	

837 [a]Recombinant wild-type (WT) or mutants EPSPS enzymes from *M. smegmatis*.

838 [b]Chromatographic column used in the first or last step of the purification protocol.

839

840

841 **Table 3.** Apparent steady-state kinetic parameters for *Ms*EPSPS
842 enzymes.

***Ms*EPSPS Enzymes**[a]	K_m **(μM)**	k_{cat} **(s^{-1})**	k_{cat}/K_m **($M^{-1}s^{-1}$)**
WT	88 ± 11	0.5530 ± 0.0185	6.28 E+03 ± 813
D61W	1014 ± 975	0.1075 ± 0.0608	1.06 E+02 ± 118
R134A	3676 ± 1007	0.1843 ± 0.0330	5.01 E+01 ± 16
E321N	3081 ± 808	0.4378 ± 0.0469	1.42 E+02 ± 40

843 [a]Recombinant EPSPS enzymes from *M. smegmatis*: WT and point mutants. S3P 844
was used at saturating concentrations (Supplemental Material – Table S1) and 845 PEP
as a variable substrate in the enzymatic assay. All reactions were performed 846 in
duplicate.

847

848

849 **Figure 1**

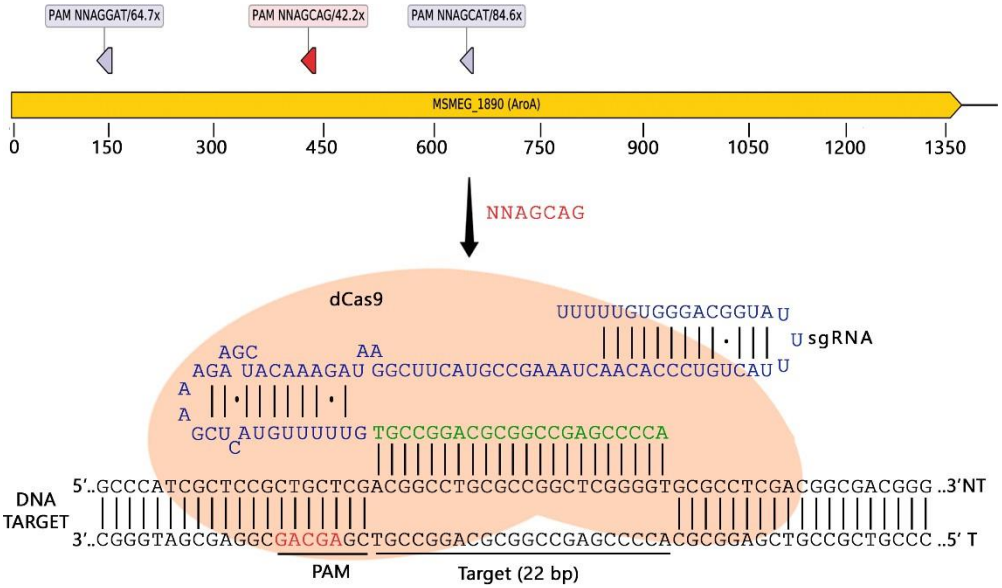

850

851

852 **Figure 2.**

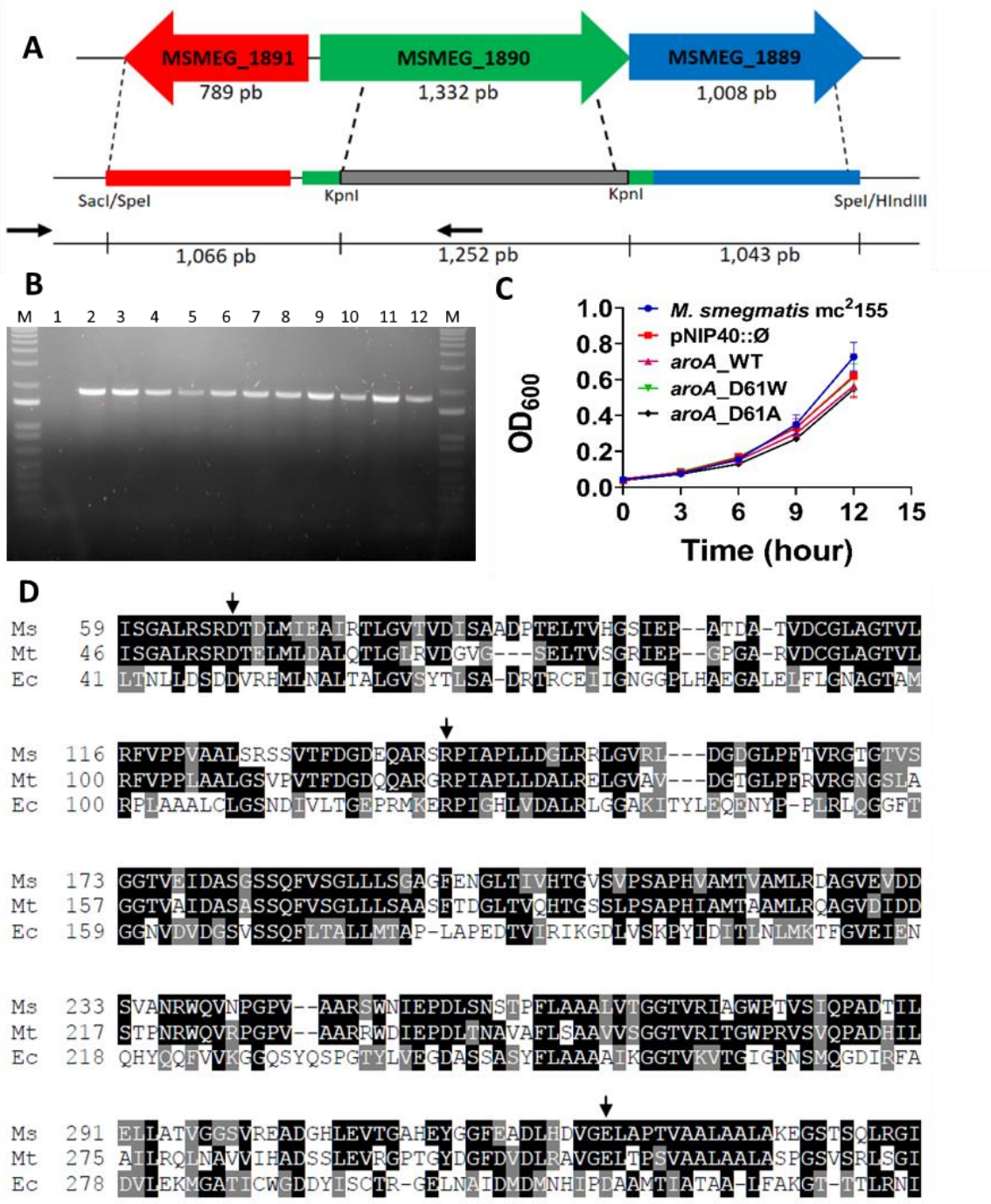

853

854

855

856

857

858

859 **Figure 3.**

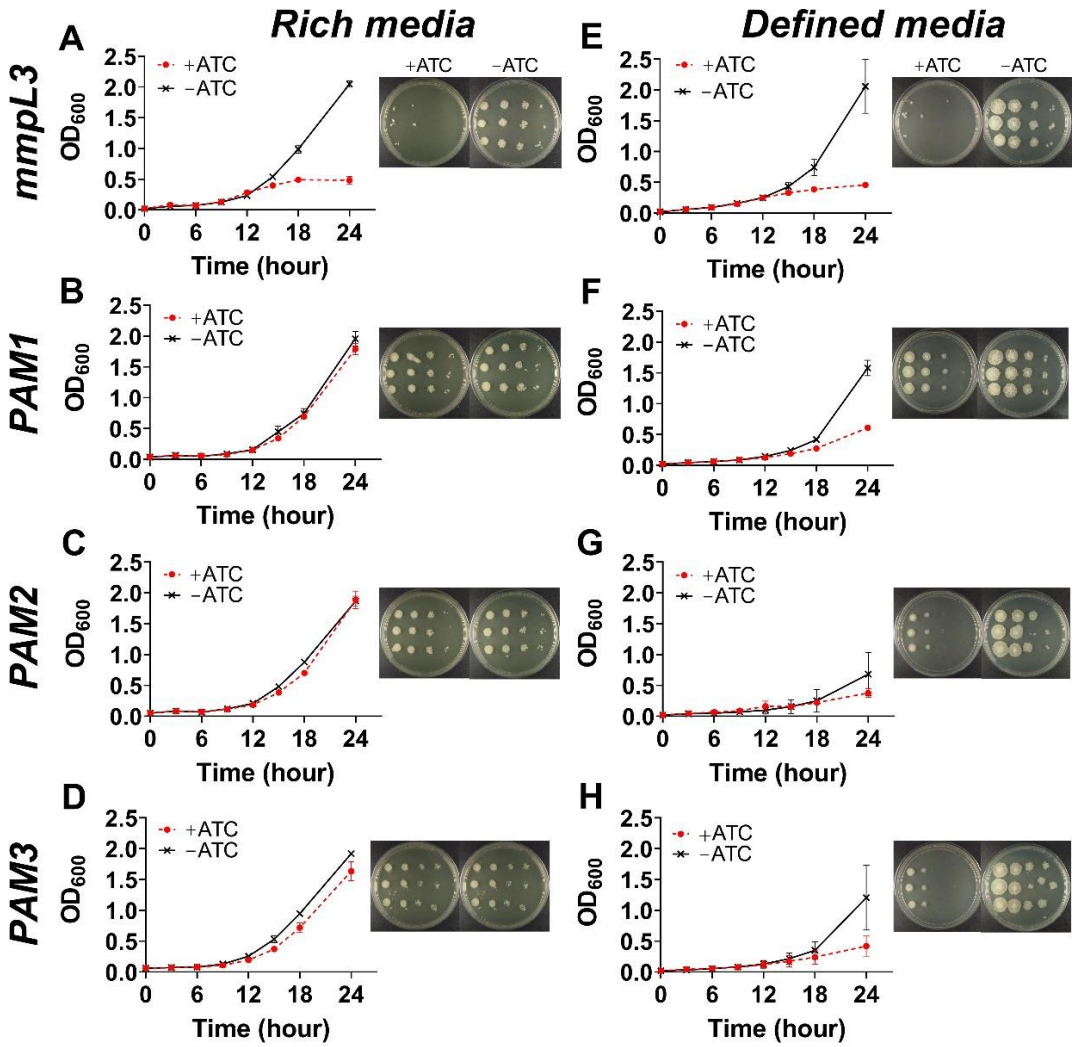

860

861

862 **Fig 4.**

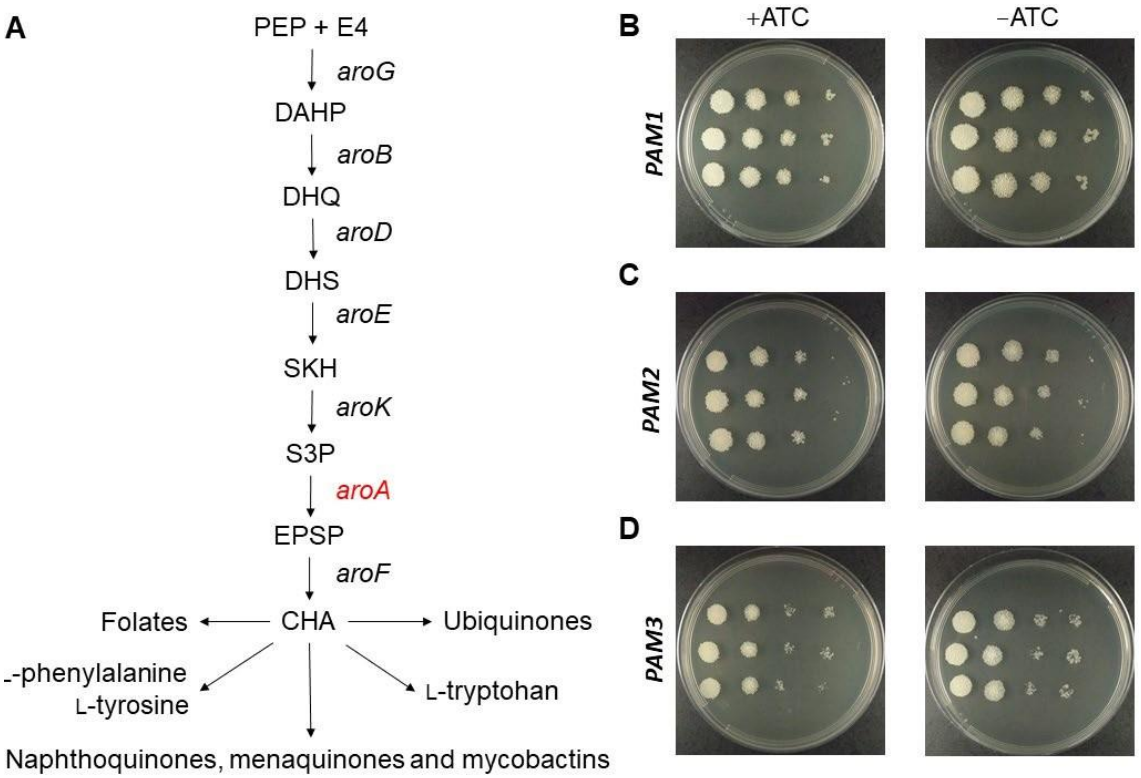

863

864

Supplemental Material

MESG

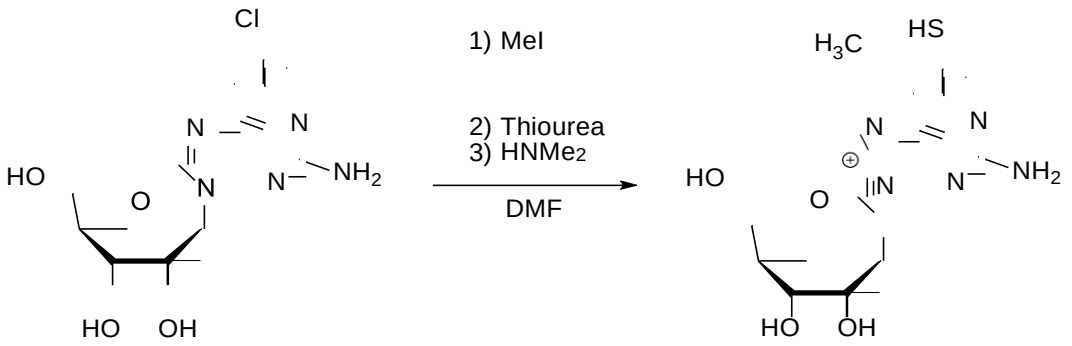

Figure S1. MESG synthesis. In a two-neck round bottom flask, under argon atmosphere, 6-chloro-guanine riboside (4.00 g, 13.25 mmol) was dissolved in dry dimethylformamide (10 mL). Then, methyl iodide (4 mL, 64.25 mmol) was added and the mixture was stirred overnight at 30 °C. Excess methyl iodide was removed under vacuum together with part of DMF. Then, to the residual mixture thiourea (2.00 g, 26.27 mmol) was added under an argon atmosphere and the mixture was stirred for an additional hour. Afterwards, the solution was neutralized with pure dimethylamine slowly added dropwise. The mixture was directly poured into stirred acetone (500 mL) to give a yellow precipitate which was further chromatographed in silica eluted with ethyl acetate/1-propanol/water (5:2:1; v/v) yielding 0,620g (30%) of **MESG**. The compound was dried to a yellow solid and stored desiccated at -80 °C. ^{13}C NMR (D_2O) δ (ppm): 174.2, 156.0, 146.6, 141.1, 119.6, 90.8, 86.2, 75.1, 70.1, 61.3, 35.4. HRMS (ESI): calc. for $[C_{11}H_{16}N_5O_4S+H]^+$: 314.0918; obt: 314.0916.[1]

Supplementary Results

MESG synthesis. High-resolution mass spectra (HRMS) were obtained on an LTQ Orbitrap Discovery mass spectrometer (Thermo Fisher Scientific). This system combines an LTQ XL linear ion-trap mass spectrometer and an Orbitrap mass analyzer. The analyses were performed through the direct infusion of the sample in MeOH/H_2O (1:1) with 0.1% formic acid (flow rate 10 mL/min) in a positive-ion mode using electrospray ionization (ESI). For elemental composition, calculations used the specific tool included in the Qual Browser module of Xcalibur (Thermo Fisher Scientific, release 2.0.7) software. ^{13}C NMR spectra were acquired on an Avance III HD Bruker spectrometer (Pontifical Catholic University of Rio Grande do Sul); chemical shifts (δ) were expressed in parts per million (ppm) relative to TMS used as an internal standard.

899 **Table S1.** Fixed and varying concentrations of substrates used in
900 kinetic assays of *Ms*EPSPS.

EPSPS	Substrate	Fixed-saturating (μM)	Substrate	Varying range (μM)
WT	S3P	800	PEP	25 - 900
D61W	S3P	600	PEP	25 - 1200
E321N	S3P	600	PEP	25 - 10000
R134A	S3P	600	PEP	300 - 2900

901

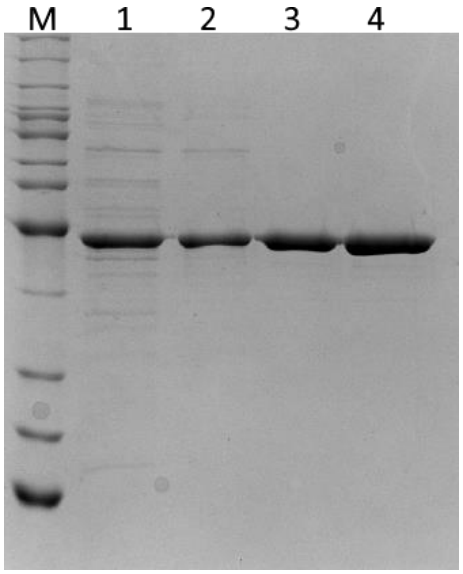

902

903 **Figure S2.** Representative SDS-PAGE from the purification steps of *Ms*EPSPS. Lane M: 904 BenchMark Protein Leadder (Invitrogen). Lane 1: crude extract from soluble fraction of cell 905 disruption. Lane 2: soluble fraction from the first column (Q-Sepharose Fast Flow). Lane 3: soluble 906 fraction from the second column (Phenyl Sepharose HP) and Lane 4: soluble fraction from the 907 third column (Mono Q HR 16/10).

908

909

910

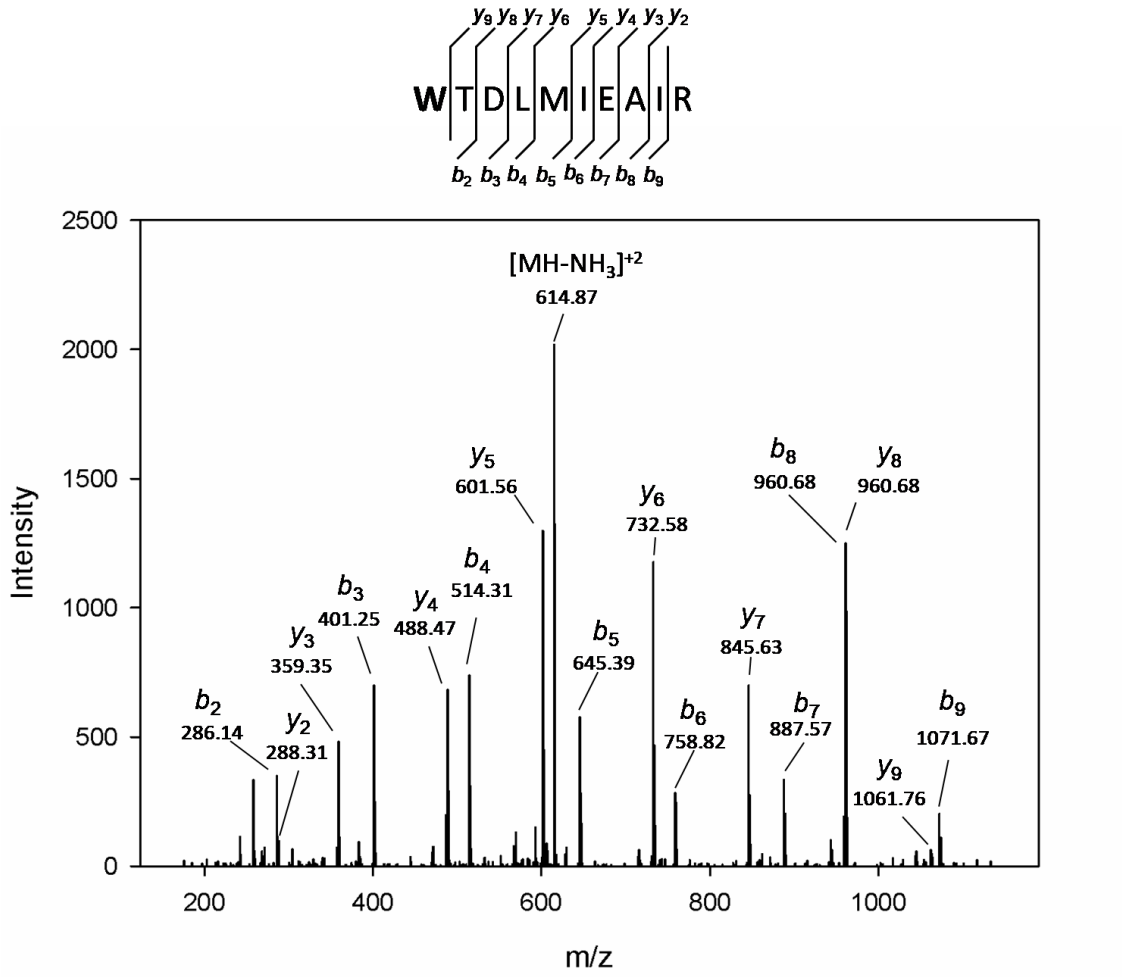

911

912 **Figure S3.** Representative spectra of peptide containing the D61W mutation obtained by LC- 913 MS/MS of *Ms*EPSPS D61W protein. Peptide sequence: **W**TDLMIEAIR. Point mutation marked in 914 **bold**. Fragment b- and y-ions and their neutral loses are indicated.

915

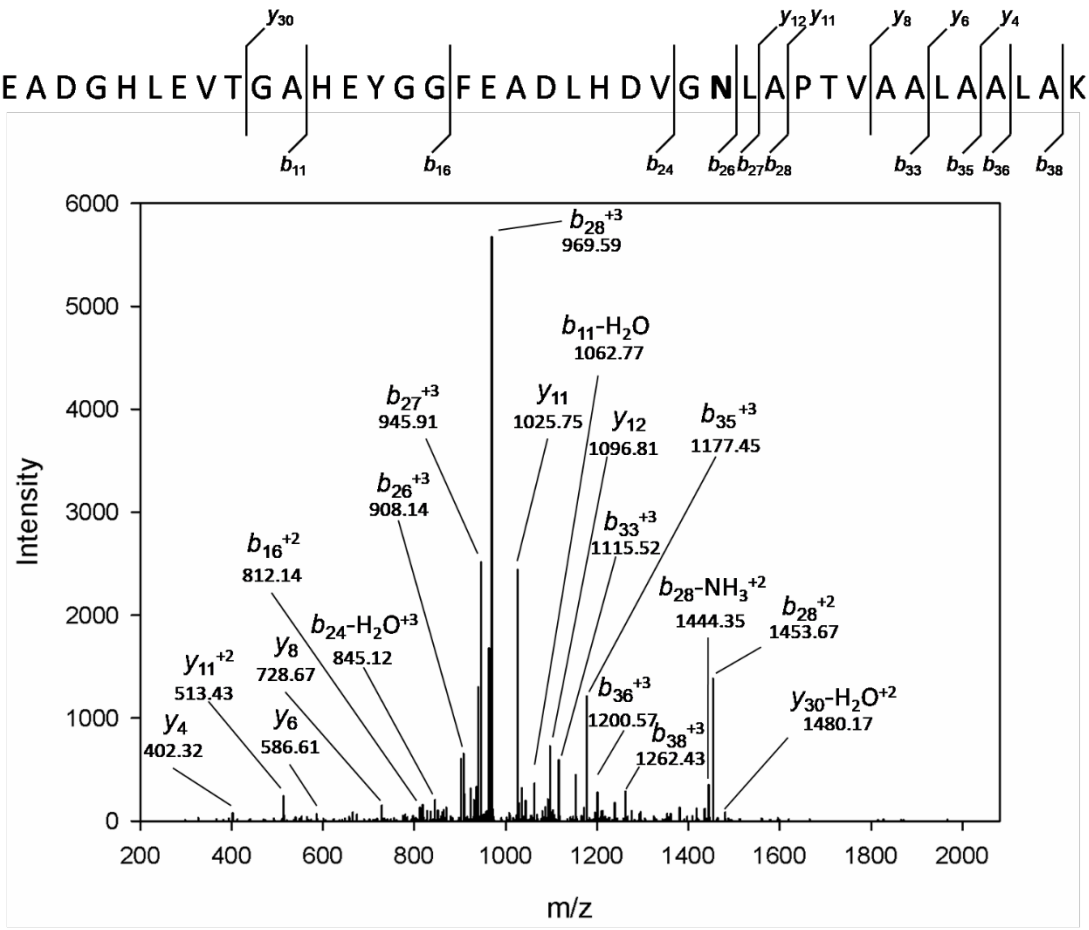

916

917 **Figure S4.** Representative spectra of peptide containing the E321N mutation obtained by LC- 918 MS/MS of *Ms*EPSPS E321N protein. Peptide sequence: EADGHLEVTGAHEYGGFEADLHDVG 919 **N**LAPTVAALAALAK. Point mutation marked in **bold**. Fragment b- and y-ions and their neutral 920 loses are indicated.

921

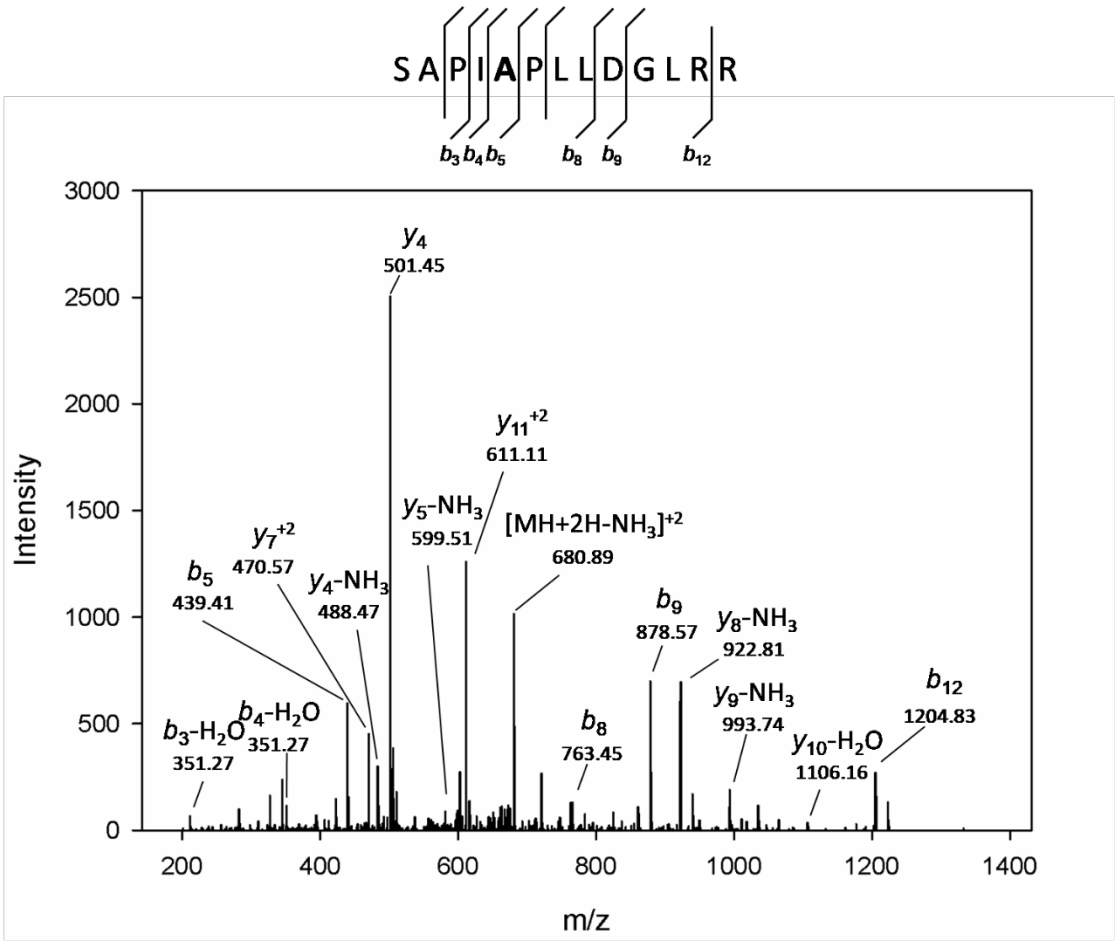

922

923

924 **Figure S5.** Representative spectra of peptide containing the R134A mutation obtained by LC- 925 MS/MS of *Ms*EPSPS R134A protein. Peptide sequence: S**A**PIAPLLDGLRR. Point mutation 926 marked in **bold**. Fragment b- and y-ions and their neutral loses are indicated.

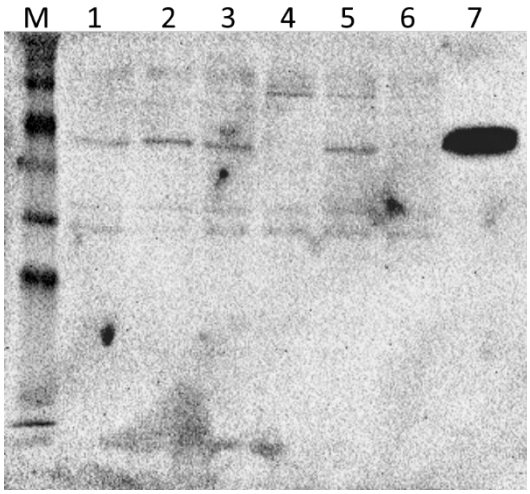

927

928 **Figure S6**. Representative Western Blot from the CRISPRi system, silencing *Ms*EPSPS. Lane 929 M: ProSieve® Color Protein Markers (Lonza). Lane 1-2: PAM1 (1) and PAM3 (2) without induction 930 with ATC (0h). Lanes 3-4: PAM1 18h after induction without (3) and with (4) ATC. Lanes 5-6: 931 PAM3 18h after induction without (5) and with (6) ATC. Lane 7: purified *Ms*EPSPS as positive 932 control.

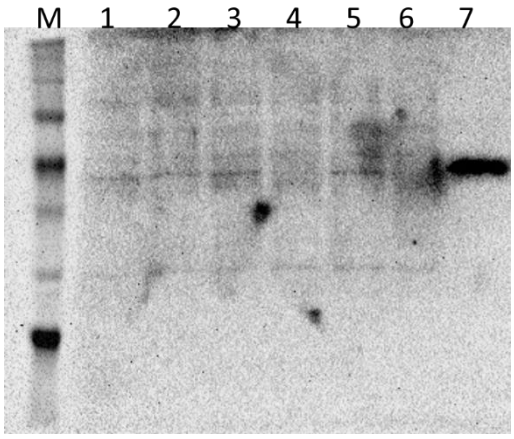

933

934 **Figure S7**. Representative Western Blot from the CRISPRi system, silencing *Ms*EPSPS. Lane 935 M: ProSieve® Color Protein Markers (Lonza). Lane 1-2: duplicate of 0h (without ATC induction) 936 for PAM2. Lanes 3 and 5: duplicate of PAM2 without ATC after 18h. Lanes 4 and 6: duplicate for 937 PAM2 after 18h of induction with ATC. Lanes 7 purified *Ms*EPSPS as positive controls.

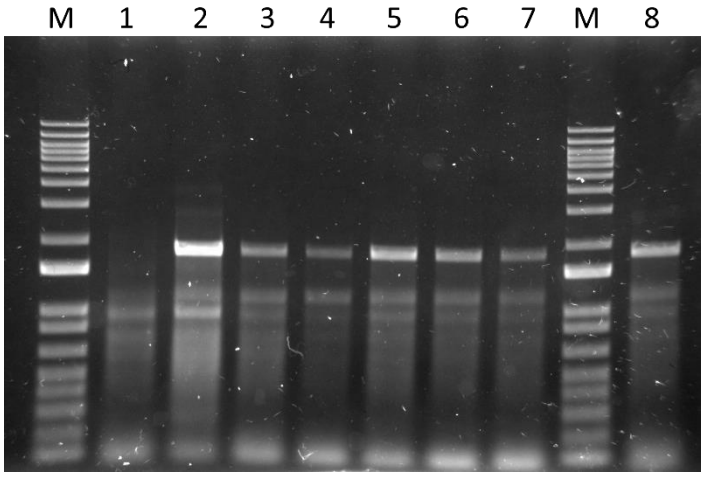

938

939 **Figure S8.** PCR confirming the interruption of the *aroA* gene produced in defined media (7H10), 940 carrying the WT, D61A, or D61W mutant copies. Genomic DNA extracted from white colonies, 941 and a pair of primers specific for the interrupted gene were used for this reaction. A band of 1,813 942 bp was expected for allelic exchange mutants. Lane M: 1kb plus DNA ladder (Invitrogen). Lane 943 1: *M. smegmatis* mc²155 genomic DNA (negative control). Lanes 2-6: strains carrying the WT 944 copy of *aroA* gene. Lane 7-8: strains carrying the D61A and D61W mutant copies of *aroA* gene. 945

5 CONSIDERAÇÕES FINAIS

O presente trabalho explorou diferentes áreas do desenvolvimento de fármacos utilizando a estratégia do alvo para o fármaco (*target to drug)* por meio de experimentos de nocaute, cinetica enzimatica e vulnerabilidade gênica. Nos últimos anos, estas ferramentas têm sido utilizadas para promover um melhor entendimento da função e validade de alvos moleculares no contexto biológico. Neste estudo, avaliamos a essencialidade do gene *aroA*, por meio de experimentos de nocaute gênico, e a vulnerabilidade da proteína por ele codificada, a enzima EPSP sintase, por meio de experimentos de *knockdown* gênico com o sistema CRISPR interference (CRISPRi).

Adicionalmente, estudamos a função do gene *aroA* e da proteína EPSPS por meio de mutantes pontuais. Entendemos que essa ferramenta pode fornecer informações valiosas e complementares às estratégias de *knockdown* gênico no processo de validação de alvos moleculares, apesar de ainda ter sido pouco explorada para essa finalidade na área de TB. Estudos de mutagênese sítio-direcionada podem revelar variantes enzimáticas que apresentem propriedades catalíticas alteradas em relação à enzima selvagem (WT). Tomemos como exemplo um mutante pontual que apresente uma eficiência catalítica (k_{cat}/K_m) reduzida quando comparada à da enzima WT. Espera-se que uma linhagem bacteriana deficiente no alelo selvagem e portando o alelo mutante que codifica para essa variante enzimática apresente uma deficiência parcial na função dessa proteína, de forma análoga ao esperado de um experimento de *knockdown* gênico com inibição incompleta de expressão. Desse modo, entendemos que o uso combinado dessas duas estratégias pode nos auxiliar no entendimento da vulnerabilidade de um alvo molecular. No caso do gene *aroA*, tema desse trabalho, observamos que mutações que apenas reduziram parcialmente a atividade da enzima *Ms*EPSPS *in vitro* (R134A e E321N) foram letais para *M. smegmatis*, sugerindo que essa enzima de fato seja um alvo vulnerável nas micobactérias. Estes resultados foram complementados pela análise de vulnerabilidade por *knockdown* gênico com o sistema CRISPRi, que também apontaram para essa enzima como um alvo vulnerável, quando as micobactérias foram crescidas em meio de cultivo definido (líquido – 7H9; sólido – 7H10), na ausência de suplementação com aminoácidos aromáticos.

Nossos resultados reforçam a noção de que, assim como a essencialidade, a vulnerabilidade não deve ser entendida como um conceito absoluto, mas sim

totalmente dependente das condições experimentais específicas, em particular da composição de nutrientes dos meios de cultivo. Mostramos de maneira clara que não existe alteração no padrão de crescimento de *M. smegmatis* após *knockdown* (KD) do gene *aroA* quando essas bactérias são cultivadas em meio rico (LB), o que caracteriza um produto gênico não vulnerável. Entretanto, em meio definido (7H9/7H10) e na ausência de suplementação com aminoácidos aromáticos, observa-se uma clara perturbação do crescimento bacteriano, caracterizando um alvo vulnerável. Mostramos que a suplementação do meio 7H9 ou 7H10 com aminoácidos aromáticos foi suficiente para promover o crescimento bacteriano sob ação do sistema de repressão sobre o gene *aroA*, mostrando que essas linhagens KD passaram a apresentar auxotrofia pelos aminoácidos aromáticos. Sugere-se, como perspectiva, avaliar tanto a essencialidade como a vulnerabilidade do gene *aroA* sob outras condições nutricionais mais variadas. Essa forte dependência da vulnerabilidade com as condições de cultivo deve servir de alerta sobre as limitações dos modelos usados para validação de alvos, uma vez que pouco se conhece em termos quantitativos a respeito do microambiente do bacilo durante a infecção. Uma perspectiva interessante desse trabalho consiste em expandir a análise de vulnerabilidade para modelos de cultura de macrófagos e de infecção em camundongos, utilizando o próprio bacilo *Mycobacterium tuberculosis*.

As técnicas implantadas durante a realização desse estudo poderão ser aplicadas a outras enzimas da via do Chiquimato, possibilitando uma visão sistêmica de quais enzimas da via apresentam maior potencial para investirmos em desenvolvimento de novos fármacos por meio do planejamento racional de análogos de substratos, produtos ou ainda estados de transição. Do mesmo modo, outras vias metabólicas também poderão ser exploradas com essas ferramentas. Adicionalmente, as técnicas de *knockdown* gênico poderão ser usadas não apenas no processo de validação de alvos, mas também de triagem fenotípica de bibliotecas químicas com células intactas. Nessa estratégia, células com níveis reduzidos de uma proteína-alvo por meio de *knockdown*, juntamente com controles com o sistema CRISPRi inativo, são usadas em triagens por compostos capazes de inibir o crescimento bacteriano. A proposta consiste em identificar compostos hits com baixa ou nenhuma capacidade de inibir o crescimento bacteriano quando a proteína-alvo se encontra expressa nos níveis normais, mas que promove esse efeito de inibição quando essa mesma proteína se encontra em níveis reduzidos. Em outras palavras, o knockdown gênico é

usado para construir cepas hipersensíveis a compostos que interajam com a proteína-alvo. Esses compostos hits poderão então representar pontos de partida para aprimoramentos por meio de química medicinal, que eventualmente poderão levar a descoberta de novos agentes anti-TB.

REFERÊNCIAS

1. Daniel TM. The history of tuberculosis. Respir Med. 2006;100(11):1862–70.
2. Warren RM, Richardson M, Sampson SL, Van Der Spuy GD, Bourn W, Hauman JH, et al. Molecular evolution of *Mycobacterium tuberculosis*: Phylogenetic reconstruction of clonal expansion. Tuberculosis. 2001;81(4):291–302.
3. Cambau E, Drancourt M. Steps towards the discovery of *Mycobacterium tuberculosis* From Ancient Times to the Discovery of the Tubercle Bacillus. Clin Microbiol Infect [Internet]. 2014;20:196–201. Available from: https://ac.els-cdn.com/S1198743X14608569/1-s2.0-S1198743X14608569-main.pdf?_tid=27ec4494-d621-11e7-b4b2-00000aacb361&acdnat=1512082535_792ec06224a8e0bb31c38b77af53f51c
4. Coban AY, Uzun M, Bozdogan B. Evaluation of agar-based medium with sheep sera for testing of drug susceptibility of *Mycobacterium tuberculosis* to Isoniazid, Rifampin, Ethambutol, and streptomycin. J Clin Microbiol [Internet]. 2013 Dec 1 [cited 2018 Jul 4];51(12):4243–5. Available from: http://www.ncbi.nlm.nih.gov/pubmed/24131699
5. Organization WH. Global Tuberculosis Report 2109. Zhurnal Eksp i Teor Fiz [Internet]. 2019 [cited 2020 Jan 27];1–134. Available from: http://apps.who.int/bookorders.
6. Chaves AS, Rodrigues MF, Mattos AMM, Teixeira HC. Challenging *Mycobacterium tuberculosis* dormancy mechanisms and their immunodiagnostic potential. Brazilian J Infect Dis [Internet]. 2015;19(6):636–42. Available from: http://dx.doi.org/10.1016/j.bjid.2015.08.004
7. WHO. GLOBAL TUBERCULOSIS REPORT 2018 [Internet]. 2018. Available from: http://apps.who.int/bookorders.
8. Cook GM, Berney M, Gebhard S, Heinemann M, Cox RA, Danilchanka O, et al. Physiology of Mycobacteria [Internet]. Vol. 55, Advances in Microbial Physiology. 2009 [cited 2018 Jul 4]. p. 81–319. Available from: http://www.ncbi.nlm.nih.gov/pubmed/19573696
9. Brown-Elliott BA, Richard J. Wallace J. Clinical and Taxonomic Status of Pathogenic Nonpigmented or Late-Pigmenting Rapidly Growing Mycobacteria Clinical and Taxonomic Status of Pathogenic Nonpigmented or Late-Pigmenting Rapidly Growing Mycobacteria. Clin Microbiol Rev. 2002;15(4):716–46.
10. Gupta RS, Lo B, Son J. Phylogenomics and comparative genomic studies robustly support division of the genus Mycobacterium into an emended genus Mycobacterium and four novel genera. Front Microbiol. 2018 Feb 13;9(FEB).
11. Pai M, Behr MA, Dowdy D, Dheda K, Divangahi M, Boehme CC, et al. Tuberculosis. Nat Rev Dis Prim. 2016;2.
12. Lou M, Burger SK, Gilpin ME, Gawuga V, Capretta A, Berti PJ. Transition state analysis of enolpyruvylshikimate 3-phosphate (EPSP) synthase (AroA)-catalyzed EPSP hydrolysis. J Am Chem Soc. 2012;134(31):12958–69.
13. Mostorides SM, Ochler RL, Grecne JN, Sinnott IV JT, Kranik M, Samlin RL. The detection of airborne *Mycobacterium tuberculosis* using micropore membrane air sampling and polymerase chain reaction. Chest [Internet]. 1999;115(1):19–25. Available from: http://dx.doi.org/10.1378/chest.115.1.19
14. Cambier CJ, Falkow S, Ramakrishnan L. Host evasion and exploitation schemes of *Mycobacterium tuberculosis*. Cell [Internet]. 2014;159(7):1497–509. Available from: http://dx.doi.org/10.1016/j.cell.2014.11.024
15. Blumberg HM, Ernst JD. The Challenge of Latent TB Infection. Jama.

2016;316(9):931–3.
16. Kana BD, Karakousis PC, Parish T, Dick T. Future target-based drug discovery for tuberculosis? Tuberculosis. 2014;94(6):551–6.
17. Getahun H, Matteelli A, Abubakar I, Abdel Aziz M, Baddeley A, Barreira D, et al. Management of latent *Mycobacterium tuberculosis* infection: WHO guidelines for low tuberculosis burden countries. Eur Respir J. 2015;46(6):1563–76.
18. Zhang Y, Yew WW. STATE OF THE ART Mechanisms of drug resistance in *Mycobacterium tuberculosis*. 2009;13(11):1320–30.
19. Boritsch EVAC, Brosch R. Evolution of *Mycobacterium tuberculosis*: New Insights into Pathogenicity and Drug Resistance. Microbiol Spectr [Internet]. 2016;4(5):1–20. Available from: http://www.asmscience.org/content/journal/microbiolspec/10.1128/microbiolspec.TBTB2-0020-2016
20. Sgaragli G, Frosini M. Human Tuberculosis II. Curr Med Chem. 2016;23:1186–216.
21. Lohrasbi V, Talebi M, Bialvaei AZ, Fattorini L, Drancourt M, Heidary M, et al. Trends in the discovery of new drugs for *Mycobacterium tuberculosis* therapy with a glance at resistance. Tuberculosis [Internet]. 2018;109(November 2017):17–27. Available from: https://doi.org/10.1016/j.tube.2017.12.002
22. Ramaswamy S, Musser JM. Molecular genetic basis of antimicrobial agent resistance in *Mycobacterium tuberculosis*: 1998 update. Tuber Lung Dis [Internet]. 1998;79(1):3–29. Available from: http://www.ncbi.nlm.nih.gov/pubmed/10645439
23. Vasconcelos IB, Meyer E, Sales F a M, Moreira IS, Basso L a, Santos DS. The mode of inhibition of *Mycobacterium tuberculosis* wild-type and isoniazid-resistant 2-trans-enoyl-ACP(CoA) reductase enzymes by an inorganic complex. Antiinfect Agents Med Chem. 2008;7(1):50–62.
24. Reingewertz TH, Meyer T, McIntosh F, Sullivan J, Meir M, Chang Y-F, et al. Differential sensitivity of mycobacteria to isoniazid is related to differences in KatG-mediated enzymatic activation of the drug. Antimicrob Agents Chemother [Internet]. 2019 Jan 27 [cited 2020 Feb 2];64(2). Available from: http://www.ncbi.nlm.nih.gov/pubmed/31767723
25. Nakata N, Kai M, Makino M. Mutation analysis of mycobacterial rpoB genes and rifampin resistance using recombinant *Mycobacterium smegmatis*. Antimicrob Agents Chemother. 2012 Apr;56(4):2008–13.
26. Zuniga ES, Early J, Parish T. The future for early-stage tuberculosis drug discovery [Internet]. Vol. 10, Future Microbiology. 2015 [cited 2018 Aug 6]. p. 217–29. Available from: www.futuremedicine.com
27. Rabahi MF, Silva Júnior JLR da, Ferreira ACG, Tannus-Silva DGS, Conde MB, Rabahi MF, et al. Tuberculosis treatment. J Bras Pneumol [Internet]. 2017 Dec [cited 2018 Aug 1];43(6):472–86. Available from: http://www.scielo.br/scielo.php?script=sci_arttext&pid=S1806-37132017000600472&lng=en&tlng=en
28. Wallis RS, Maeurer M, Mwaba P, Chakaya J, Rustomjee R, Migliori GB, et al. Tuberculosis-advances in development of new drugs, treatment regimens, host-directed therapies, and biomarkers. Lancet Infect Dis [Internet]. 2016;16(4):e34–46. Available from: http://dx.doi.org/10.1016/S1473-3099(16)00070-0
29. Bald D, Villellas C, Lu P, Koul A. Targeting energy metabolism in

Mycobacterium tuberculosis, a new paradigm in antimycobacterial drug discovery [Internet]. Rubin EJ, Collier RJ, editors. Vol. 8, mBio. 2017 [cited 2018 Jul 4]. p. e00272-17. Available from: http://www.ncbi.nlm.nih.gov/pubmed/28400527

30. Falcão VCA, Villela AD, Rodrigues-Junior VS, Pissinate K, Eichler P, Pinto AFM, et al. Validation of *Mycobacterium tuberculosis* dihydroneopterin aldolase as a molecular target for anti-tuberculosis drug development. Biochem Biophys Res Commun [Internet]. 2017 Apr 15 [cited 2018 Aug 1];485(4):814–9. Available from: https://www.sciencedirect.com/science/article/pii/S0006291X17304370?via%3Dihub
31. Dalberto PF, Rodrigues-Junior V, Almeida Falcão VC, Pinto AFM, Abbadi BL, Bizarro CV, et al. Assessing the role of deoD gene in *Mycobacterium tuberculosis* in vitro growth and macrophage infection. Microb Pathog [Internet]. 2018;119(November 2017):60–4. Available from: https://doi.org/10.1016/j.micpath.2018.03.056
32. Villela AD, Rodrigues-Junior VS, Pinto AFM, Falcão VC de A, Sánchez-Quitian ZA, Eichler P, et al. Construction of *Mycobacterium tuberculosis* cdd knockout and evaluation of invasion and growth in macrophages. Mem Inst Oswaldo Cruz [Internet]. 2017 Nov [cited 2018 Aug 1];112(11):785–9. Available from: http://www.ncbi.nlm.nih.gov/pubmed/29091140
33. Simithy J, Reeve N, Hobrath J V., Reynolds RC, Calderón AI. Identification of shikimate kinase inhibitors among anti-*Mycobacterium tuberculosis* compounds by LC-MS. Tuberculosis [Internet]. 2014;94(2):152–8. Available from: http://dx.doi.org/10.1016/j.tube.2013.12.004
34. Singh V, Mizrahi V. Identification and validation of novel drug targets in *Mycobacterium tuberculosis*. Drug Discov Today [Internet]. 2017;22(3):503–9. Available from: http://dx.doi.org/10.1016/j.drudis.2016.09.010
35. Lechartier B, Rybniker J, Zumla A, Cole ST. Tuberculosis drug discovery in the post- post-genomic era. EMBO Mol Med. 2014;6(2):1–11.
36. Lee JA, Berg EL. Neoclassic drug discovery: The case for lead generation using phenotypic and functional approaches. J Biomol Screen. 2013;18(10):1143–55.
37. Sala C, Hartkoorn RC. Tuberculosis drugs: new candidates and how to find more. Future Microbiol [Internet]. 2011 Jun;6(6):617–33. Available from: https://www.futuremedicine.com/doi/10.2217/fmb.11.46
38. DeJesus, M. A., Gerrick, E. R., Xu, W., Park, S. W., Long, J. E., Boutte, C. C. & Sassetti CM. Comprehensive Essentiality Analysis of the *Mycobacterium tuberculosis* Genome via Saturating Transposon Mutagenesis. MBio. 2017;8(1):1–17.
39. Lamrabet O, Drancourt M. Genetic engineering of *Mycobacterium tuberculosis*: A review. Tuberculosis [Internet]. 2012;92(5):365–76. Available from: http://dx.doi.org/10.1016/j.tube.2012.06.002
40. Ramachandran V, Singh R, Yang X, Tunduguru R, Mohapatra S, Khandelwal S, et al. Genetic and chemical knockdown: A complementary strategy for evaluating an anti-infective target. Adv Appl Bioinforma Chem. 2013;6(1):1–13.
41. Rock JM, Hopkins FF, Chavez A, Diallo M, Chase MR, Gerrick ER, et al. Programmable transcriptional repression in mycobacteria using an orthogonal CRISPR interference platform. Nat Microbiol [Internet]. 2017;2(February):1–9. Available from: http://dx.doi.org/10.1038/nmicrobiol.2016.274

42. Xiao J, Jia H, Pan L, Li Z, Lv L, Du B, et al. Application of the CRISPRi system to repress sepF expression in *Mycobacterium smegmatis*. Infect Genet Evol [Internet]. 2018;(June):0–1. Available from: https://doi.org/10.1016/j.meegid.2018.06.033
43. Li W, Obregón-Henao A, Wallach JB, North EJ, Lee RE, Gonzalez-Juarrero M, et al. Therapeutic potential of the *Mycobacterium tuberculosis* mycolic acid transporter, MmpL3. Antimicrob Agents Chemother. 2016 Sep 1;60(9):5198–207.
44. Herrmann KM, Weaver LM. the Shikimate Pathway. Annu Rev Plant Physiol Plant Mol Biol [Internet]. 1999;50(1):473–503. Available from: http://www.annualreviews.org/doi/10.1146/annurev.arplant.50.1.473
45. Ducati RG, Basso L a, Santos DS. Mycobacterial shikimate pathway enzymes as targets for drug design. Curr Drug Targets. 2007;8(3):423–35.
46. Rizzi C, Frazzon J, Ely F, Weber PG, Da Fonseca IO, Gallas M, et al. DAHP synthase from *Mycobacterium tuberculosis* H37Rv: Cloning, expression, and purification of functional enzyme. Protein Expr Purif. 2005;40(1):23–30.
47. Parish T, Stoker NG. The common aromatic amino acid biosynthesis pathway is essential in *Mycobacterium tuberculosis*. Microbiology [Internet]. 2002;148(Pt 10):3069–77. Available from: http://mic.microbiologyresearch.org/content/journal/micro/10.1099/00221287-148-10-3069
48. Sassetti CM, Boyd DH, Rubin EJ. Genes required for mycobacterial growth defined by high density mutagenesis. Mol Microbiol. 2003;48(1):77—84.
49. Griffin JE, Gawronski JD, DeJesus MA, Ioerger TR, Akerley BJ, Sassetti CM. High-resolution phenotypic profiling defines genes essential for mycobacterial growth and cholesterol catabolism. PLoS Pathog. 2011;7(9):1–9.
50. Marques MR, Pereira JH, Oliveira JS, Basso LA, de Azevedo, Walter Filgueira J, Santos DS, et al. The inhibition of 5-enolpyruvylshikimate-3-phosphate synthase as a model for development of novel antimicrobials. Curr Drug Targets [Internet]. 2007;8(3):445–57.
51. Peng RH, Tian YS, Xiong AS, Zhao W, Fu XY, Han HJ, et al. A novel 5-enolpyruvylshikimate-3-phosphate synthase from Rahnella aquatilis with significantly reduced glyphosate sensitivity. PLoS One. 2012;7(8):1–10.
52. Mizyed S, Wright JEI, Byczynski B, Berti PJ. Identification of the catalytic residues of AroA (Enolpyruvylshikimate 3-phosphate synthase) using partitioning analysis. Biochemistry. 2003;42(23):6986–95.
53. McDevitt D, Payne DJ, Holmes DJ, Rosenberg M. Novel targets for the future development of antibacterial agents. J Appl Microbiol [Internet]. 2002 [cited 2018 Aug 12];92 Suppl:28S-34S. Available from: http://www.ncbi.nlm.nih.gov/pubmed/12000610
54. McArthur JD, West NP, Cole JN, Jungnitz H, Guzmán CA, Chin J, et al. An aromatic amino acid auxotrophic mutant of Bordetella bronchiseptica is attenuated and immunogenic in a mouse model of infection. FEMS Microbiol Lett [Internet]. 2003 Apr 11 [cited 2018 Aug 12];221(1):7–16. Available from: http://www.ncbi.nlm.nih.gov/pubmed/12694904
55. Coggins JR, Abell C, Evans LB, Frederickson M, Robinson D a, Roszak a W, et al. Experiences with the shikimate-pathway enzymes as targets for rational drug design. Biochem Soc Trans [Internet]. 2003;31(Pt 3):548–52. Available from: http://www.biochemsoctrans.org/bst/031/bst0310548.htm
56. Steinrücken HC, Amrhein N. The herbicide glyphosate is a potent inhibitor of 5-

enolpyruvylshikimic acid-3-phosphate synthase. Biochem Biophys Res Commun [Internet]. 1980 Jun 30 [cited 2018 Aug 12];94(4):1207–12. Available from: http://www.ncbi.nlm.nih.gov/pubmed/7396959

57. Sergiev IG, Alexieva VS, Ivanov S V., Moskova II, Karanov EN. The phenylurea cytokinin 4PU-30 protects maize plants against glyphosate action. Pestic Biochem Physiol [Internet]. 2006 Jul 1 [cited 2018 Aug 13];85(3):139–46. Available from: https://www.sciencedirect.com/science/article/pii/S0048357506000022
58. Haghani K, Salmanian AH, Ranjbar B, Zakikhan-Alang K, Khajeh K. Comparative studies of wild type Escherichia coli 5-enolpyruvylshikimate 3-phosphate synthase with three glyphosate-insensitive mutated forms: Activity, stability and structural characterization. Biochim Biophys Acta - Proteins Proteomics. 2008;1784(9):1167–75.
59. Timmers LFSM, Neto AMS, Montalvão RW, Basso LA, Santos DS, Norberto de Souza O. EPSP synthase flexibility is determinant to its function: computational molecular dynamics and metadynamics studies. J Mol Model. 2017;
60. Bentley R, Haslam E. The shikimate pathway—a metabolic tree with many branches. Crit Rev Biochem Mol Biol. 1990;25(5):307–83.
61. Zucko J, Dunlap WC, Shick JM, Cullum J, Cercelet F, Amin B, et al. Global genome analysis of the shikimic acid pathway reveals greater gene loss in host-associated than in free-living bacteria. BMC Genomics [Internet]. 2010;11(1):628. Available from: http://www.biomedcentral.com/1471-2164/11/628
62. Crowther GJ, Shanmugam D, Carmona SJ, Doyle MA, Hertz-Fowler C, Berriman M, et al. Identification of attractive drug targets in neglected- disease pathogens using an in Silico approach. PLoS Negl Trop Dis. 2010;4(8).